Journal of Zoological Systematics and Evolutionary Research

WILEY

RESEARCH ARTICLE OPEN ACCESS

Integrative Taxonomy and Biogeographical History of the Subgenus *Abea*, With Synonymy of *Micronialoe* (Coleoptera: Carabidae: *Pterostichus*)

Dooyoung Kim[1,2] | Jangwon Seo[3] | Ui Wook Hwang[1,4,5,6,7]

[1]Department of Biomedical Convergence Science and Technology, School of Industrial Technology Advances, Kyungpook National University, Daegu, Republic of Korea | [2]Department of Environmental Science, Policy, and Management, University of California, Berkeley, California, USA | [3]Department of Biological Sciences and Biotechnology, Chungbuk National University, Cheongju, Republic of Korea | [4]Department of Biology Education, Teachers College and Institute for Phylogenomics and Evolution, Kyungpook National University, Daegu, Republic of Korea | [5]Department of Advanced Bioconvergence, Kyungpook National University, Daegu, Republic of Korea | [6]Institute for Korean Herb-Bio Convergence Promotion, Kyungpook National University, Daegu, Republic of Korea | [7]Phylomics Inc., Daegu, Republic of Korea

Correspondence: Ui Wook Hwang (uwhwang@knu.ac.kr)

Received: 24 September 2025 | **Revised:** 13 December 2025 | **Accepted:** 9 January 2026

Academic Editor: Yuzine Esa

Keywords: biodiversity | morphometrics | new species | phylogenetics | Pterostichini

ABSTRACT

The ground beetle subgenera *Abea* Morita and *Micronialoe* Park, Kwon & Lafer are a small group within the genus *Pterostichus*, endemic to Japan and Korea. In this study, we apply an integrative approach combining molecular and morphological evidence to resolve their taxonomic problems at subgeneric and specific levels. Phylogenetic reconstruction of *Pterostichus* and related genera using *28S rRNA* supported *Micronialoe* as a junior synonym of *Abea*. Examination of more than 250 specimens of Korean *Abea* revealed eight distinct morphotypes defined by male genitalia, despite high external morphological similarity. Phylogenetic analysis using a concatenated dataset of *28S rRNA* and *COI* recovered seven major clades within Korean *Abea*, supporting four new species: *Pterostichus subterraneus* sp. nov., *P. bifoveolatoides* sp. nov., *P. mixtus* sp. nov., and *P. multispinulosus* sp. nov. Genetic divergence analyses under the Kimura 2-parameter model revealed a barcoding gap in *28S rRNA* (0.9%–1.0%) but overlap in *COI* (1.0%–1.5%). Traditional morphometric analyses of 190 specimens, based on two raw measurements and 13 ratios, did not clearly resolve species boundaries for most species. These results underscore the importance of integrating molecular evidence and male genital morphology for species delimitation within *Abea*. Our phylogenetic framework further provided insights into subterranean adaptation and genital evolution. Additionally, time-calibrated analyses and ancestral area reconstruction suggested dispersal of *Abea* and related subgenera from China to Korea and Japan. Together, these findings provide insight into the systematics and biogeography of *Pterostichus* ground beetles.

1 | Introduction

Abea Morita, 1992 and *Micronialoe* Park, Kwon & Lafer, 1996 are subgenera of the ground beetle genus *Pterostichus* Bonelli, 1810, endemic to the Japanese Archipelago and Korean Peninsula. These are small groups, consisting of one and four described species, respectively, and are primarily associated with forest ecosystems. All species in both subgenera possess reduced hindwings, indicating flightlessness and limited dispersal ability [1, 2]. These subgenera are considered closely related, with the

primary morphological difference being the shape of the right paramere in male genitalia: slender and curved in *Micronialoe*, while stout and straight in *Abea* [2, 3]. Molecular analyses based on *28S rRNA* and wingless also support their close affinity [4]. Despite this, the taxonomic validity of *Micronialoe* has not been critically re-examined.

In South Korea, *Micronialoe* has been reported from various regions [2], but there hasn't been a detailed taxonomic examination of the specimens. A recent discovery of a new species by Kim and Suh [2] highlighted the potential for additional undescribed diversity, particularly in unstudied regional populations. In this study, we collected and examined over 250 specimens of *Micronialoe* from the southern part of the Korean Peninsula. Although some distinct differentiation was identified in the male genitalia, the similar external morphology across specimens raised further questions regarding species boundaries. Additionally, the presence of sympatric species pairs complicated accurate species identification, especially for female specimens lacking clear diagnostic features.

Molecular data have been widely used to resolve the supra- and intraspecific taxonomic problems in carabid beetles. Within the genus *Pterostichus*, the *28S rRNA* D1–D3 region has been commonly used to infer subgeneric relationships (e.g., [4–6]). For species delimitation and identification, the *COI* barcoding region has been broadly used within insects [7, 8], including *Pterostichus* [9, 10]. Additionally, Will and Gill [5] presented the possibility of three genetic markers, *COI* (3' end region), *COII*, and *28S rRNA* D1–D3, for species delimitation in the *Hypherpes* subgenus complex of *Pterostichus*.

Morphometrics can be used to identify morphological differences between closely related species. Both traditional and geometric morphometrics have been utilized for identifying interspecific differences in carabid beetles (e.g., traditional: Sasakawa and Kubota [11] and Huber and Schnitter [12]; geometric: Sasakawa [13] and Roggero et al. [14]). While traditional morphometrics can be considered a more classical method, many taxonomic keys of carabid beetles rely on raw measurement and ratio data (e.g., *Pterostichus*: Sasakawa and Mitsuduka [15]; other carabids: Habu [16]), underscoring its continuous value in taxonomic studies.

Beyond species delimitation, studying taxa with low dispersal capabilities can offer valuable insight into historical biogeography. Flightless beetles are typically more sensitive to geographic barriers, and their distributions are often confined to the place where they originated [17]. Previous phylogenetic studies in *Pterostichus* have also incorporated biogeographical approaches by comparing distribution patterns at the species-group and species levels in the context of phylogenetic frameworks (e.g., [5, 6]).

We had three main purposes for this study. First, to clarify the subgeneric classification of *Abea* and *Micronialoe*, we analyzed newly acquired and previously published sequences from the *28S rRNA* (D1–D3 region). Second, to delimit the Korean *Micronialoe* species, we employed both *28S rRNA* and *COI* genetic markers. In addition, traditional morphometric analyses were conducted to identify the morphological diagnostic characters of the newly recognized species. Finally, we explored the evolutionary and biogeographical history of *Abea* based on the phylogenetic framework. The biogeographical history of *Abea* and related subgenera was inferred through time-calibration and ancestral area reconstruction analyses.

2 | Materials and Methods

2.1 | Sample Examination

Specimens were hand-collected at the collection sites (Figure 1A). After being brought to the laboratory, their genitalia were dissected and stored in microtubes with glycerin. The specimens themselves were preserved in 99% ethanol. All examined specimens are deposited at Kyungpook National University (KNU, Daegu-si, Korea). The habitus and male genitalia were observed and photographed under a stereoscopic microscope (Leica M205C), and the female genitalia under a compound microscope (Leica DM 2500). Then, we preliminarily classified the specimens into morphotypes based on male genitalia.

Abbreviations for localities are presented as follows: Gyeonggi-do (GG); Gangwon-do (GW); Gyeongsangbuk-do (GB); Gyeongsangnam-do (GN); Chungcheongbuk-do (CB); Chungcheongnam-do (CN); Jeollabuk-do (JB); Jeollanam-do (JN); Daegu-si (DG); Ulsan-si (US); Busan-si (PS). The maps used in this study were retrieved from a free map-providing site (https://d-maps.com) and modified using Adobe Illustrator v22.2.

2.2 | Measurements

Measurements were taken as follows: body length from the anterior margin of the clypeus to the apex of elytra (BL); head width across the eyes (HW); pronotum width along the widest point (PW); basal width of pronotum between the basal angles (PbW); apical width of pronotum between the apical angles (PaW); pronotum length along the median line (PL); elytral width along the widest point (EW); elytral width between humeri (EbW); elytral length from the basal border near scutellum to the apex (EL).

2.3 | DNA Extraction, PCR, and Sequencing

Total genomic DNA was extracted from the genital apparatus or mesofemur of the specimens using the DNeasy Blood and Tissue Kit (Qiagen, Germany) according to the manufacturer's instructions. Gene fragments of ~1050 bp from the *28S rRNA* D1–D3 region were amplified using D1-5′ GGGAGGAAAAGAAACTAAC 3′ [18] and D3i-5′ GCATAGTTCACCATCTTTC 3′ [5], and ~650 bp from the *COI* barcoding region were amplified using LCO1490-5′ GGTCAACAAATCATAAAGATATTGG 3′ and HCO2198-5′ TAAACTTCAGGGTGACCAAAAAATCA 3′ [19]. PCRs were performed in a 50 μL mixture containing 5 μL of 10× Taq DNA polymerase reaction buffer, 1 μL of 10 mM dNTP mix, 2 μL of 10 pM of each primer, 0.25 μL of 5 U/μL DiaStar Taq DNA polymerase, and 1 μL of genomic DNA. The thermal cycling conditions were as follows: initial denaturation at 94°C for 2 min; 35 cycles of denaturation at 94°C for 20 s, annealing at 48–52°C for 40 s, and extension at 72°C for 1 min; followed by a final extension at 72°C for 5 min. PCR products were sequenced using a 3730 DNA sequencer (PerkinElmer, USA) at Solgent Co. (Daejeon, Korea). The sequence data generated in this study have been deposited in GenBank under accession numbers PV954984–PV955010 and PV955577–PV955597.

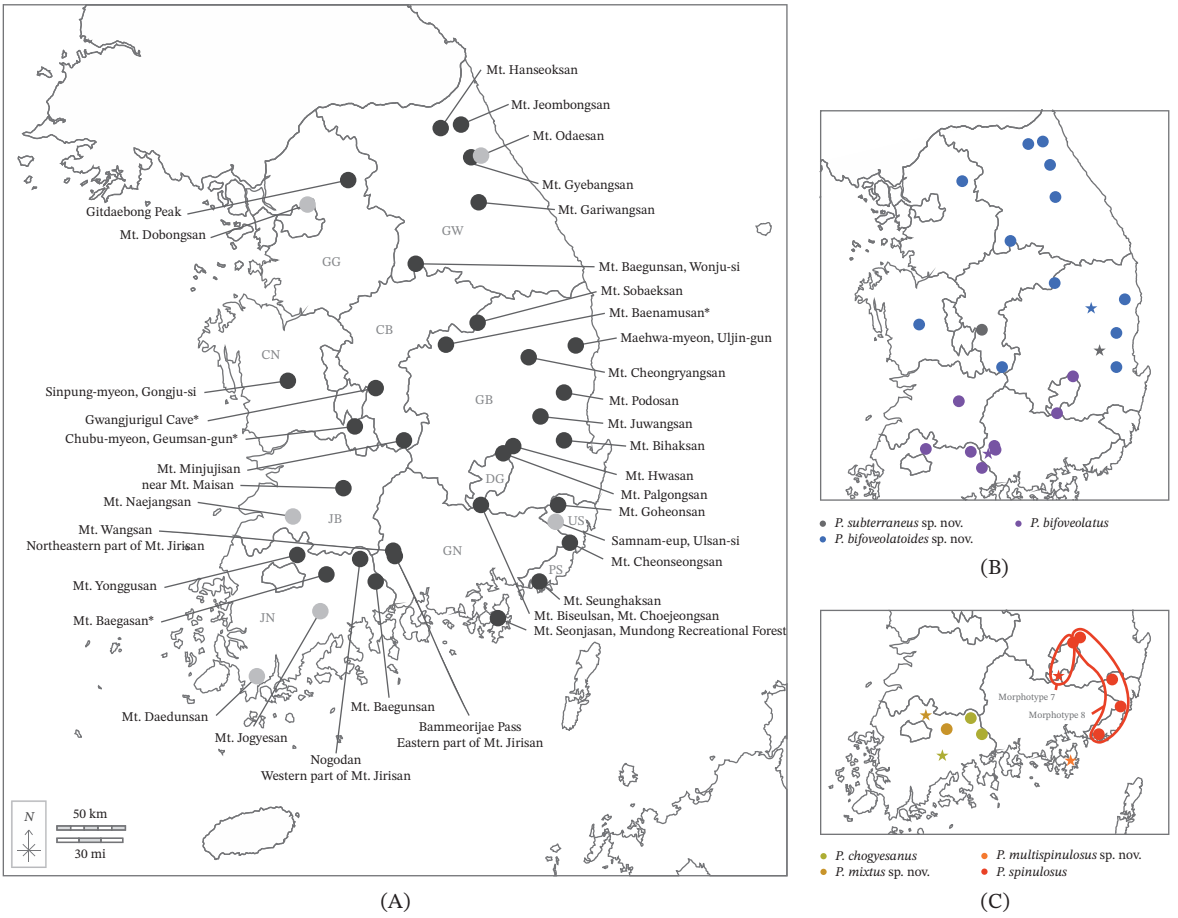

FIGURE 1 | Collection sites (A) and identification results (B, C) for the Korean *Abea* species. (A) Collection sites from this study (dark gray) and previous records (light gray). Asterisk (*) indicates localities where only female specimens were collected. (B) Confirmed localities of *P. subterraneus*, *P. bifoveolatoides*, and *P. bifoveolatus*. (C) Confirmed localities of *P. chogyesanus*, *P. mixtus*, *P. multispinulosus*, and *P. spinulosus*. Stars indicate the type locality of each species.

2.4 | Sequence Alignment

Four datasets (Supporting Information 1: Table S1) were used for phylogenetic analyses: *28S rRNA* dataset of the genus *Pterostichus* (Dataset 1); *28S rRNA* dataset of *Abea*, *Micronialoe*, and related subgenera (Dataset 2); *28S rRNA* and *COI* concatenated dataset of Korean *Micronialoe* (Dataset 3); *COI* dataset of Korean *Micronialoe* (Dataset 4). For Datasets 1 and 2, sequence data were compiled from previous studies in addition to the data generated in this study [4–6, 18, 20–22].

COI sequences were aligned using the Clustal-X algorithm [23] implemented in BioEdit 7.2.5 [24]. For *28S rRNA*, alignments were performed using MAFFT [25] with the L-INS-i search option for Dataset 1, and Q-INS-i for Datasets 2 and 3. The start and end points of the sequences were trimmed manually in BioEdit. Poorly aligned regions of *28S rRNA* were excluded using a modified GBLOCKS algorithm [26] implemented in MESQUITE v3.81 [27]. Exclusion criteria followed Kavanaugh et al. [28] with the following parameters: minimum fraction of identical residues for a conserved position = 0.2; minimum fraction of identical residues for a highly conserved position = 0.4; counting fraction within only those taxa that have non-gaps at that position; maximum length of contiguous non-conserved blocks = 4; minimum length of a block = 4; and allowed fraction of gaps within a position = 0.5.

2.5 | Phylogenetic Analyses

Maximum likelihood (ML) analysis was performed using W-IQ-TREE [29], partitioning the dataset by gene for the concatenated dataset. The best-fit substitution models for each gene were determined using ModelFinder [30] in W-IQ-TREE, selected based on the Bayesian Information Criterion (BIC) as TVM+F+I+G4 for *28S rRNA* and TIM+F+G4 for *COI*. An edge-unlinked partition model [31] was employed for the concatenated dataset, and ultrafast bootstrap support [32] was assessed with 1000 iterations.

Bayesian inference (BI) analyses were conducted using MrBayes 3.2.7a [33] for Dataset 3, employing an edge-unlinked partition model with substitution models of GTR+I+G4 for *28S rRNA* and GTR+G4 for *COI*. The analysis was run for 50 million generations with two runs of four chains each, sampling every 1000 generations and discarding the first 25% as burn-in. After the runs, the average standard deviation of split frequencies was 0.001500, indicating convergence between independent runs. All model parameters exhibited adequate sampling, with effective sample sizes exceeding 200 and a potential scale reduction factor of 1.000 for all parameters, further confirming convergence.

Preliminary divergence time estimation was conducted using BEAST2 [34], with the *Pterostichus* clade roughly calibrated at 35–42 million years ago (Ma) following Schmidt et al. [6]. For

TABLE 1 | Genetic distances (%) among *Abea*, *Micronialoe*, and related subgenera based on *28S rRNA* sequences, calculated using the Kimura 2-parameter (K2P) model.

	Micronialoe							*Abea*	*Georgeballius*	*Sinosteropus*	*Circinatus*	Outgroup
	***P. subterraneus* (Morphotype 1)**	***P. bifoveolatoides* (Morphotype 2)**	***P. bifoveolatus* (Morphotype 3)**	***P. chogyesanus* (Morphotype 4)**	***P. mixtus* (Morphotype 5)**	***P. multispinulosus* (Morphotype 6)**	***P. spinulosus* (Morphotypes 7 + 8)**	***P. yamauchii***				***P. sulcitarsis***
P. subterraneus	0.0	—	—	—	—	—	—	—	—	—	—	—
P. bifoveolatoides	2.6–2.8	0.0–0.8	—	—	—	—	—	—	—	—	—	—
P. bifoveolatus	2.6–2.9	2.0–2.6	0.1–**0.9**	—	—	—	—	—	—	—	—	—
P. chogyesanus	3.0	2.1–2.2	2.2–2.8	0.0	—	—	—	—	—	—	—	—
P. mixtus	**3.4**	2.3	2.7–3.2	1.7	0.0	—	—	—	—	—	—	—
P. multispinulosus	3.3	2.3–2.4	2.5–3.2	1.5	1.8	—	—	—	—	—	—	—
P. spinulosus	3.2–3.3	2.0–2.3	2.4–3.1	**1.0**–1.1	1.6–1.7	1.7–1.8	0.0–0.1	—	—	—	—	—
P. yamauchii	1.7	2.0	1.7–2.0	2.7	3.0	3.0	2.8–2.9	—	—	—	—	—
Georgeballius	3.7–3.8	4.7–5.1	4.3–4.9	4.6.4.8	5.0–5.2	5.1–5.3	4.8–5.0	4.0–4.3	0.3	—	—	—
Sinosteropus	3.3–3.7	4.5–4.9	4.1–4.6	4.1–4.4	4.3–5.0	4.7–4.9	4.5–5.1	3.8–4.1	**2.3**–2.8	0.6–1.3	—	—
Circinatus	5.8	5.9–6.0	6.0–6.2	6.3	6.8–6.9	6.4	**7.0**	6.1	5.7–5.9	5.2–5.5	0.0	—
P. sulcitarsis	9.1	8.6–8.7	8.9–9.2	9.3	9.5	9.1	9.3	8.5	9.3–9.6	8.3–8.4	8.4	—

Note: Rows 1–7 represent interspecific and intraspecific genetic distances among *Micronialoe* species, with bold numbers corresponding to one of the following: the lowest interspecific, highest interspecific, or highest intraspecific genetic distance. Row 8 represents the genetic distances between *Abea* and *Micronialoe*. Rows 9–11 represent intersubgeneric and intrasubgeneric genetic distances, with bold numbers indicating the lowest or highest intersubgeneric distances. The final row represents the genetic distances between the five subgenera and an outgroup.

calibration, we included an early branching member of *Pterostichus*, the subgenus *Argutor* Dejean, according to previous phylogenetic studies ([4]; Figure S1 of [6]). Divergence times were estimated under the birth-death model [35] with an uncorrelated lognormal relaxed clock [36] and the GTR + G4 substitution model. A lognormal distribution was applied for the calibration prior. The analysis was run for 50 million generations with a 10% burn-in period. Convergence was assessed by effective sample sizes (ESS > 200 for all parameters) using Tracer v1.7.2 [37]. Maximum clade credibility trees were summarized using TreeAnnotator v2.7.6, with node heights set as common ancestor heights. All trees were visualized through FigTree v1.4.4. [38].

The ancestral area estimation of *Abea*, *Micronialoe*, and relatives was conducted via the Bayesian Binary MCMC (BBM) method in RASP 3.2 [39], using the tree file generated by BEAST2 as input. For the RASP analysis, we divided the study area into the following biogeographical regions: (i) China, (ii) Korea, and (iii) northeast Japan. The distribution data for the included subgenera were compiled from previous studies [6, 40–42].

2.6 | Genetic Distance Calculation

Genetic distances were calculated using MEGA 12 [43] with the Kimura 2-parameter model [44] for both the *28S rRNA* (Dataset 2) and *COI* (Dataset 4) datasets. These distances were used to evaluate inter- and intrasubgeneric as well as inter- and intraspecific variation. The pairwise distance dataset was processed and visualized as histograms in R v4.4.2 [45] using R Studio v2023.09.1 [46], with the ggplot2 [47], tidyr [48], and dplyr [49] packages.

2.7 | Morphometric Analyses

For morphometric analyses, we obtained two raw morphological measurements (BL and EW) and 13 ratios (BL/EL, PW/HW, PW/PL, PW/PbW, PW/PaW, PbW/PaW, P widest, P seta, EW/PW, EL/PL, EL/EW, EW/EbW, and PW/EbW), from 190 individuals (2 individuals for *P. subterraneus*, 36 for *P. bifoveolatoides*, 52 for *P. bifoveolatus*, 19 for *P. chogyesanus*, 7 for *P. mixtus*, 14 for *P. multispinulosus*, and 60 for *P. spinulosus*) (Supporting Information 2: Table S2). "P widest" represents the ratio of the distance from the pronotal apex to the widest point over the pronotal length. "P seta" represents the ratio of the distance from the pronotal apex to the pronotal seta over the pronotal length. Species classification followed phylogenetic results, regarding Morphotypes 7 and 8 as a single species. Female specimens were included through identification based on pronotal shape and punctures (more details under the identification key section). Female specimens that could not be identified confidently were all excluded from the analysis.

Before the morphometric analyses, we checked whether variables had significant differences between sexes. Overall, we had only a few female specimens for most examined species, so we tested the statistical difference for a single species, *P. bifoveolatoides*, which included 31 males and 21 females. Either the *t*-test (for variables that follow normal distributions) or the Wilcoxon test (for variables that do not follow normal distributions) indicated that there are no significant differences between sexes for the compared variables. Therefore, we conducted the analyses including both sexes.

The morphometric analyses were performed in R v4.4.2 using R Studio v2023.09.1. Boxplots were visualized using the ggplot2,

tidyr, and dplyr packages. Principal component analysis (PCA) was performed on the full dataset and visualized using ggplot2. Linear discriminant analysis (LDA) was performed using the *lda* function from the MASS [50] with groupings based on phylogenetic results and visualized through ggplot2. *Pterostichus subterraneus* was excluded from the LDA due to insufficient sample size ($n = 2$). To explore morphological differentiation among closely related species, LDA was first performed on six species and repeated by sequentially removing well-separated species. This stepwise approach aimed to reveal fine-scale morphological patterns that may be masked by the inclusion of the morphologically distinct taxa.

3 | Results

3.1 | Subgeneric Relationships

Our ML tree based on *28S rRNA* sequences (910 bp) from the genus *Pterostichus* and related taxa (Figure 2A, Dataset 1) revealed that *Pterostichus* is paraphyletic. This paraphyly results from the subgenus *Bothriopterus*, *P.* cf. *migliaccioi*, and *P. deuvesianus* being positioned outside the main clade, while the genera *Cyclotrachelus* and *Tapinopterus* were placed within the main clade. The genus *Poecilus* was a sister group to the main clade of *Pterostichus*. The so-called "modern *Pterostichus* (sensu [6])" was a sister group to the clade comprising *Argutor*, *Badistrinus*, and *Phonias*. *Abea* and *Micronialoe* were closely related to *Circinatus*, *Sinosteropus*, and *Georgeballius* with a strong bootstrap support value (BP = 93). Besides, several clades of *Pterostichus* were strongly supported as monophyletic (BP > 92): *Hypherpes* complex, *Ethira* complex, *Nialoe* complex (sensu lato), *Platysma* + *Metallophilus*, *Pterostichus* s. str + *Platypterus* + *Oreophilus*, and *Lyrothorax* + *Melanius* + *Lamenius*.

An additional ML tree was constructed using 1,039 bp of *28S rRNA* sequences (Figure 2B, Dataset 2), focusing on *Abea*, *Micronialoe*, and related subgenera. It consistently revealed *Abea* to be placed within the *Micronialoe* clade (BP = 99). Besides, *Sinosteropus* and *Georgeballius* formed a sister group relationship (BP = 85), and *Circinatus* formed a sister group to the rest of the subgenera in this group.

In the genetic distance analysis based on the Kimura 2-parameter (K2P) model for *28S rRNA* (Table 1, Figure 2C), intersubgeneric divergences among *Abea*, *Micronialoe*, *Georgeballius*, *Sinosteropus*, and *Circinatus* ranged from 3.3% to 7.0%, except for two subgenera pairs: (i) *Abea* and *Micronialoe*: 1.7%–3.0%; (ii)

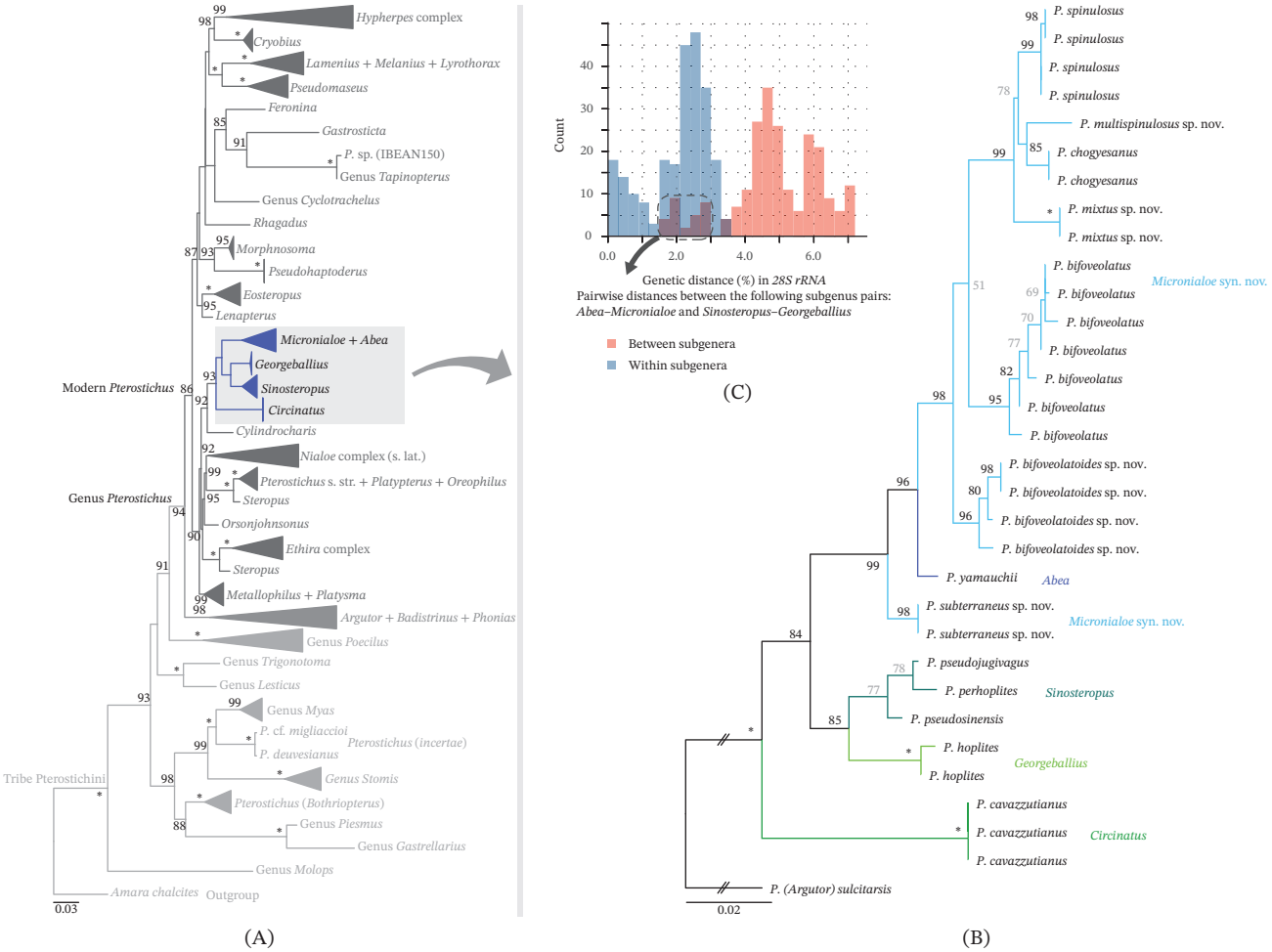

FIGURE 2 | Phylogenetic analyses of the genus *Pterostichus* based on *28S rRNA* sequences. (A) Maximum likelihood tree of the genus *Pterostichus*. (B) Maximum likelihood tree of *Abea*, *Micronialoe*, and related subgenera. Numbers on nodes represent bootstrap support values (BP), with full support marked by an asterisk (*), and values below 80 are omitted (A) or shown in gray (B). (C) Distribution of intra- and intersubgeneric genetic distances among *Abea*, *Micronialoe*, and related subgenera. based on the Kimura 2-parameter model for *28S rRNA* sequences.

Georgeballius and *Sinosteropus*: 2.3%–2.8% (Figure 2C). In contrast, the largest intrasubgeneric divergence was observed within *Micronialoe* as 3.4%. Based on phylogenetic relationships and genetic divergences, we suggest *Micronialoe* syn. nov. as a junior synonym of *Abea* (detailed explanation given in "Discussion").

3.2 | Morphotypes of Korean *Abea*

Through examination of male genitalia, eight morphotypes of *Abea* were identified across the southern Korean Peninsula (Table 2). Among them, morphotypes 3, 4, and 7 correspond to the previously reported species: *P. bifoveolatus*, *P. chogyesanus*, and *P. spinulosus*. The remaining five morphotypes were newly identified through this study.

3.3 | Korean *Abea* Phylogeny

The ML and BI trees based on concatenated *28S rRNA* (1,037 bp) and *COI* (626 bp) sequences from 21 *Abea* specimens (Figure 5A, Dataset 3) revealed seven well-supported, monophyletic clades (BP > 99; BPP = 1). Each clade corresponded to a distinct male genital morphotype, except for one (Morphotype 8), which was nested within the *P. spinulosus* clade. We named the remaining four morphotypes as follows: Morphotype 1: *P. subterraneus* sp. nov.; 2: *P. bifoveolatoides* sp. nov.; 5: *P. mixtus* sp. nov.; 6: *P. multispinulosus* sp. nov. (Table 2).

The subterranean-adapted species, *P. subterraneus*, was shown to be a sister group to the remaining, and the epigean species formed the monophyletic clade (BP = 98; BPP = 1.00). Species with only the gonoporal piece and ventral sclerite in the median lobe of the aedeagus, *P. subterraneus*, *P. bifoveolatoides*, and *P. bifoveolatus* (Figure 5A, Table 2), did not form a monophyletic clade. *Pterostichus bifoveolatus* and *P. bifoveolatoides* were shown to be closely allied with moderate support values (BP = 66; BPP = 0.81), primarily differing in the presence of a carina in the median lobe of the aedeagus. The remaining four species, *P. chogyesanus*, *P. mixtus*, *P. multispinulosus*, and *P. spinulosus*, formed a monophyletic clade (BP = 82; BPP = 1.00). The ML tree supported the monophyly of the species with the spiny patch in the median lobe of the aedeagus: *P. mixtus*, *P. multispinulosus*, and *P. spinulosus* (Table 2), while the BI tree resulted in a polytomy for three clades, including *P. chogyesanus*, *P. mixtus*, and the clade of *P. multispinulosus* + *P. spinulosus*.

The ML tree based on 626 bp of *COI* sequences of 27 Korean *Abea* specimens (Figure 6A, Dataset 4) consistently supported *P. subterraneus* as an early diverging species within the subgenus. Unlike the results based on the concatenated dataset (Figure 5A), *P. chogyesanus* was shown to be a sister group to all remaining epigean species. The close relationship between *P. bifoveolatus* and *P. bifoveolatoides* was supported with a low support value (BP = 46). The monophyly of the species with the spiny patch in the median lobe of the aedeagus (*P. mixtus*, *P. multispinulosus*, and *P. spinulosus*) was supported (BP = 59), but *P. multispinulosus* was nested within the clade of *P. spinulosus*.

In the genetic divergence analyses, interspecific distances of *28S rRNA* ranged from 1.0% to 3.4%, while intraspecific values reached up to 0.9% (Table 1, Figure 5B). For *COI* barcoding sequences among the Korean *Abea* species (Table 3, Figure 6B), interspecific distances ranged from 2.8% to 8.0%, except for the species pair between *P. multispinulosus* and *P. spinulosus*

TABLE 2 | Character states of morphotypes and subsequent classification of the Korean *Abea* species.

Characters in median lobe of the aedeagus		Morphotypes							
		1	2	3	4	5	6	7	8
Apex	Shape	Round	Round	Round	Round	Nearly truncate	Truncate	Truncate	Truncate
Gonopore piece (GP)	Presence	Present	Present	Present	Present	Present	Present	Present	Present
Ventral sclerite (VS)	Presence	Present	Present	Present	Absent	Present	Present	Present	Present
	Size	Medium	Medium	Large	N/A	Medium	Small	Small	Small
	Shape	Triangular	Oval	Triangular	N/A	Oval	Oval	Narrow	Narrow
Spiny patch (SP)	Presence	Absent	Absent	Absent	Absent	Present	Present	Present	Present
	Numbers	N/A	N/A	N/A	N/A	1	3	1	1
	Location	N/A	N/A	N/A	N/A	Subapical side	Dorsal and subapical side	Dorsal side	Subapical side
Carina (C)	Presence	Absent	Absent	Present	Absent	Present	Present	Present	Present
References		Figure 3A–E	Figure 3F–J	Figure 4A–J	Kim and Suh [2]	Figure 3K–O	Figure 3P–T	Kim and Suh [2]	Figure 4K–T
Classification		*P. subterraneus* sp. nov.	*P. bifoveolatoides* sp. nov.	*P. bifoveolatus*	*P. chogyesanus*	*P. mixtus* sp. nov.	*P. multispinulosus* sp. nov.	*P. spinulosus* Kim and Suh	*P. spinulosus* Kim and Suh

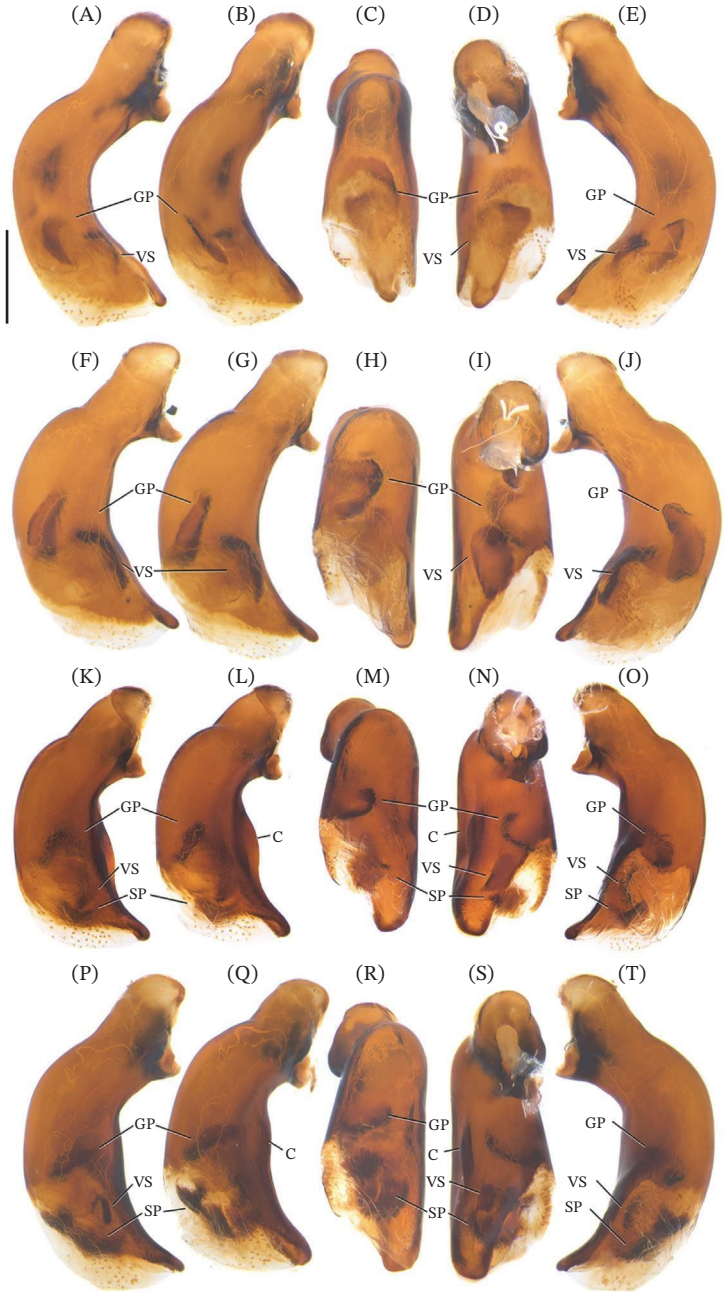

FIGURE 3 | Median lobe of the aedeagus of four *Abea* species. (A–E) *P. subterraneus* sp. nov. (F–J) *P. bifoveolatoides* sp. nov. (K–O) *P. mixtus* sp. nov. (P–T). *P. multispinulosus* sp. nov. Right lateral view (A, F, K, P); dorsolateral view (B, G, L, Q); dorsal view (C, H, M, R); ventral view (D, I, N, S); left lateral view (E, J, O, T). Scale bar: 0.3 mm. C, ventral carina; GP, gonopore piece; SP, spiny patch; VS, ventral sclerite.

(1.0%–1.3%). The species with high intraspecific distances were *P. subterraneus* (1.5%) and *P. bifoveolatus* (up to 1.0%).

3.4 | Morphometric Analyses

3.4.1 | Boxplots of Korean *Abea* Species

Boxplots (Figure 7A), based on the raw measurements and ratios of 190 specimens (2 individuals for *P. subterraneus*, 36 for *P. bifoveolatoides*, 52 for *P. bifoveolatus*, 19 for *P. chogyesanus*, 7 for *P. mixtus*, 14 for *P. multispinulosus*, and 60 for *P. spinulosus*), revealed morphometric variation among Korean *Abea* species. *Pterostichus subterraneus* and *P. chogyesanus* appeared to be morphometrically distinct from the others. For example, *P. subterraneus* had the longest elytra relative to pronotal length (EL/PL), and a wide pronotal base relative to pronotal width (PW/PbW). *Pterostichus chogyesanus*, the smallest Korean *Abea* species, was also characterized by a wide head relative to the pronotum (PW/HW) and a narrow pronotal base relative to pronotal width (PW/PbW).

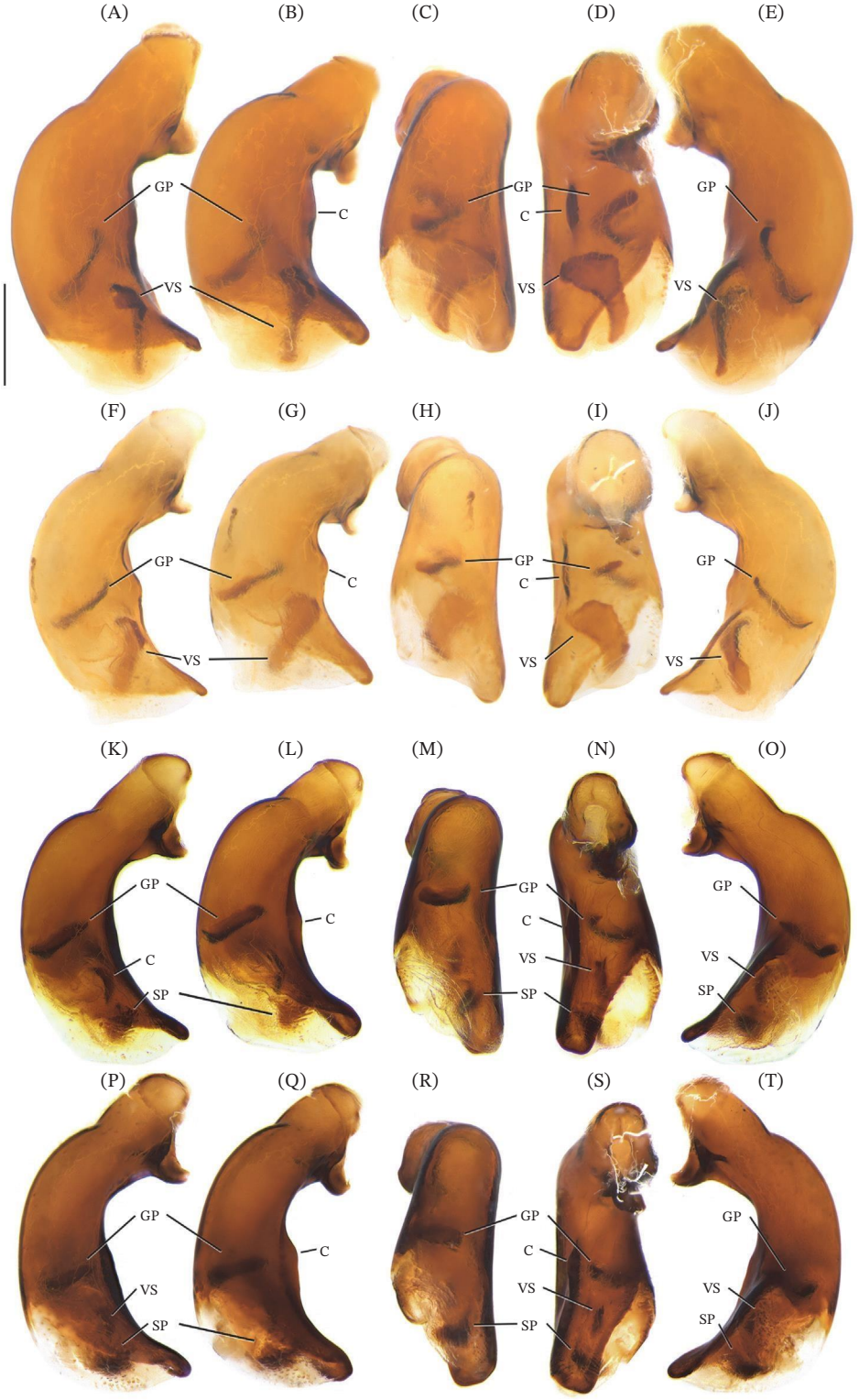

FIGURE 4 | Median lobe of the aedeagus of two *Abea* species. (A–E) *P. bifoveolatus* from the western part of Mt. Jirisan (JN). (F–J) Ditto from Mt. Wangsan (GN). (K–O) *P. spinulosus* from Mt. Hwasan (GB). (P–T) Ditto from Mt. Goheonsan (GN). Right lateral view (A, F, K, P); dorsolateral view (B, G, L, Q); dorsal view (C, H, M, R); ventral view (D, I, N, S); left lateral view (E, J, O, T). Scale bar: 0.3 mm. C, ventral carina; GP, gonopore piece; SP, spiny patch; VS, ventral sclerite.

3.4.2 | Multivariate Morphometric Analyses of Korean *Abea* Species

The PCA ordination based on two raw measurements and 13 ratios (Figure 7B) showed partial separation among the seven species. The first nine principal components (PC) were required to explain 95% of the total variance (Supporting Information 3: Table S3), suggesting that morphological variation was distributed across many dimensions and PCA was not ideal for dimensionality reduction in this dataset. PC1 was driven by

BL, EW/EbW, and EW, while PC2 was influenced by PW/PaW, EL/PL, and PW/EbW. *Pterostichus chogyesanus* (green) formed a relatively distinct cluster on the right side of the plot, corresponding to high PC1 values, influenced by EW/EbW, PW/PbW, and EW/PW. *Pterostichus subterraneus* (gray) appeared on the bottom-left side of the plot, which is affected by EL/EW, EL/PL, and BL/EW. *Pterostichus bifoveolatus* (blue) overlapped with other species near the center, but showed relative separation from the others by BL, BL/EW, EL/EW, and EL/PL. In contrast, *P. bifoveolatoides* (purple), *P. mixtus* (gold), *P. multispinulosus* (orange), and *P. spinulosus* (red) occupied a broad central cloud of intermediate PC1/PC2 values.

The first LDA (Figure 7C) was based on six species, excluding *P. subterraneus* due to insufficient data ($n = 2$). The first two linear discriminants (LD1 and LD2) together explained 88.05%

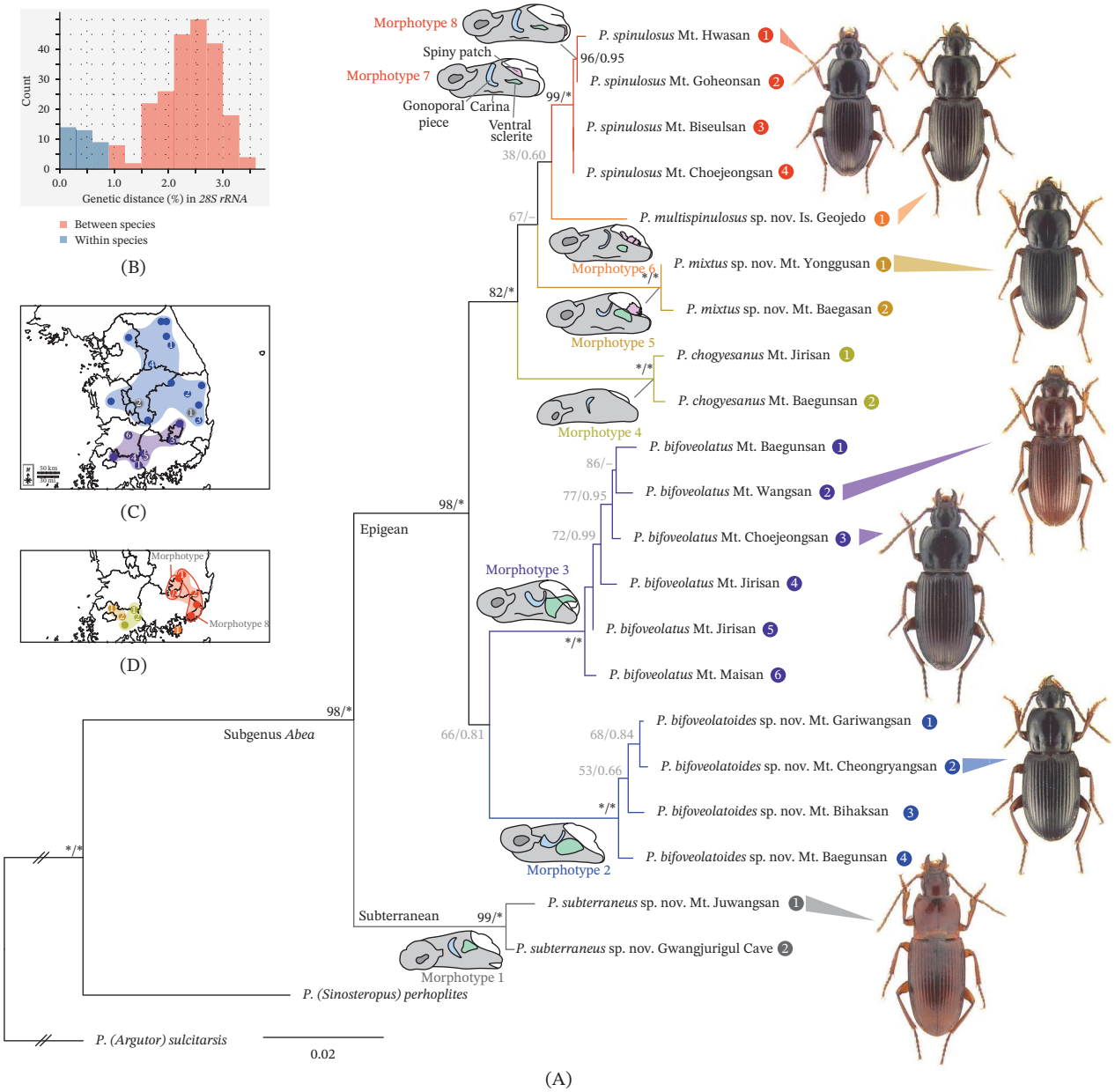

FIGURE 5 | Phylogenetic analyses of the Korean *Abea* based on *28S rRNA* and *COI* sequences. (A) Maximum likelihood tree based on concatenated dataset of *28S rRNA* and *COI* sequences. Numbers on nodes represent bootstrap support values (BP) and bayesian posterior probabilities (BPP). Fully supported values are marked by an asterisk (*), and BP values below 80 are shown in gray. Genital morphotypes associated with each corresponding node are illustrated in ventral view. (B) Distribution of intra- and interspecific genetic distances among analyzed species based on the Kimura 2-parameter model for *28S rRNA* sequences. (C, D) The distribution information for each species. Circles represent collection localities, with numbers corresponding to localities of the sequence data in the phylogenetic tree.

TABLE 3 | Genetic distances (%) among Korean *Abea* species based on *COI* sequences, calculated using the Kimura 2-parameter (K2P) model.

	P. subterraneus (Morphotype 1)	*P. bifoveolatoides* (Morphotype 2)	*P. bifoveolatus* (Morphotype 3)	*P. chogyesanus* (Morphotype 4)	*P. mixtus* (Morphotype 5)	*P. multispinulosus* (Morphotype 6)	*P. spinulosus* (Morphotypes 7 + 8)
P. subterraneus	**1.5**	—	—	—	—	—	—
P. bifoveolatoides	6.7–7.4	0.0–0.8	—	—	—	—	—
P. bifoveolatus	5.8–6.9	4.1–5.3	0.2–1.0	—	—	—	—
P. chogyesanus	6.5–7.2	5.5–6.4	4.3–5.2	0.8	—	—	—
P. mixtus	6.9–**8.0**	4.6–5.5	4.8–5.5	5.3–5.7	0.5	—	—
P. multispinulosus	5.8–6.5	4.7–5.2	3.6–4.3	4.6–4.8	3.8	—	—
P. spinulosus	4.8–5.7	3.6–4.1	3.3–4.0	4.0–4.3	2.8–3.1	**1.0**–1.3	0.0–0.3

Note: The bold numbers correspond to one of the following: The lowest interspecific, the highest interspecific, or the highest intraspecific genetic distance.

of the total variance. LD1 was mainly influenced by PW/EbW, EW/PW, and EW/EbW, while LD2 was affected by PW/PbW, PW/PaW, and PbW/PaW (Supporting Information 4: Table S4). *Pterostichus chogyesanus* formed a well-separated cluster on the top-left quadrant, and *P. bifoveolatus* was positioned on the top-right, with some overlap near the center of the plot. Other species overlapped more broadly, although *P. bifoveolatoides* was separated from *P. spinulosus*, and *P. mixtus* was distinguishable from *P. multispinulosus* in general.

In the second LDA (Figure 7D), *P. chogyesanus* was excluded, resulting in five species being analyzed. LD1 and LD2 accounted for 85.86% of the total variance, with both axes primarily influenced by EW/PW, PW/EbW, and EW/EbW (Supporting Information 4: Table S4). *Pterostichus bifoveolatus* formed a cluster on the right side of the plot, while some data were close or overlapped with the remaining three species. The separations between *P. bifoveolatoides* and *P. spinulosus*, as well as *P. mixtus* and *P. multispinulosus*, became more evident.

The third LDA plot (Figure 7E) was based on four species, which additionally excluded *P. bifoveolatus*. LD1 and LD2 together explained 88.90% of the total variance. LD1 was influenced by PW/PL, PW/PbW, and EL/EW, while LD2 was again affected by EW/PW, PW/EbW, and EW/EbW (Supporting Information 4: Table S4). Similar separation patterns for the two species pairs were still supported, but *P. bifoveolatoides* and *P. spinulosus* exhibited overlap near the middle. *Pterostichus multispinulosus* was consistently located between the aforementioned species pair.

3.5 | Phylogeographical Analyses

The time-calibrated tree based on *Abea* and related subgenera (Figure 8A, Dataset 2) indicated that *Circinatus* and the clade of *Sinosteropus*, *Georgeballius*, and *Abea* diverged in the late Oligocene (26.9 Ma; 95% HPD, 15.8–38.4 Ma). *Abea* and the clade of *Sinosteropus* + *Georgeballius* diverged in the early Miocene (20.3 Ma; 95% HPD, 10.6–31.4 Ma). The Japanese *Abea* clade diverged from the Korean clade around the late Miocene (11.0 Ma; 95% HPD, 5.2–17.8 Ma), and *Sinosteropus* (mainly distributed in China) and *Georgeballius* (endemic to Japan) diverged around a similar period (10.7 Ma; 95% HPD, 4.0–18.6 Ma). The RASP indicated that *Abea* and related subgenera originated in China with a possible dispersal toward Korea and Japan.

4 | Discussion

4.1 | Subgeneric Relationships

Our reconstructed ML tree of the genus *Pterostichus* and its relatives (Figure 2A) revealed paraphyly of *Pterostichus*, consistent with Schmidt et al. [6]. Our support of the clade encompassing *Abea*, *Micronialoe*, *Georgeballius*, *Sinosteropus*, and *Circinatus* is consistent with Schmidt et al. [6]. Additionally, monophyly was consistently supported for the following subgeneric groupings, as in Sasakawa and Kubota [4] and Schmidt et al. [6]: *Platysma* + *Metallophilus*, *Pterostichus* s. str + *Platypterus* + *Oreophilus*, *Lyrothorax* + *Melanius* + *Lamenius*, and *Argutor* + *Badistrinus* + *Phonias*. The subgenus *Bothriopterus* was placed outside of the major clade of the genus *Pterostichus*, and monophyly of both the

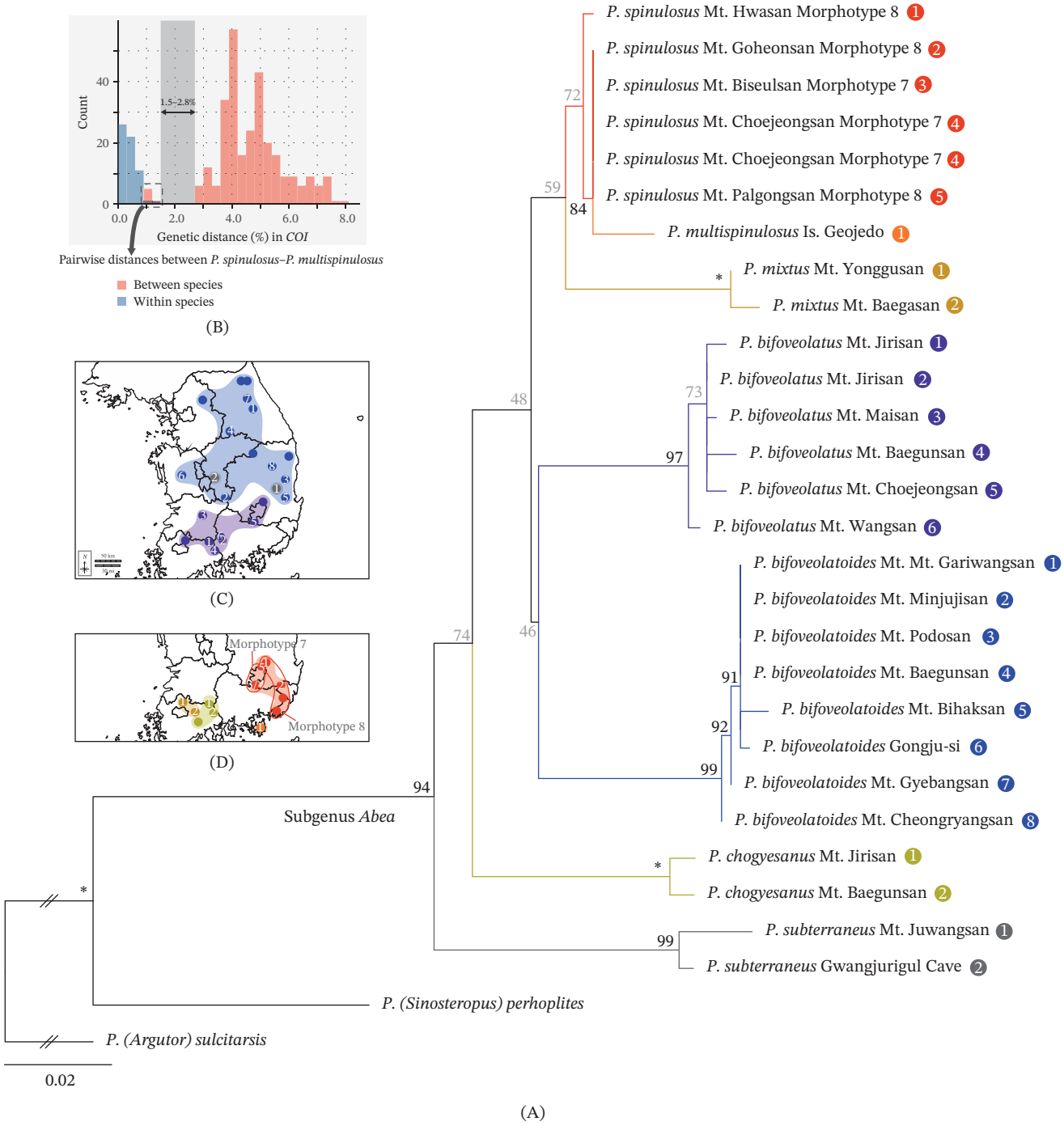

FIGURE 6 | Phylogenetic analyses of Korean *Abea* species based on *COI* sequences. (A) Maximum likelihood tree. Numbers on nodes represent bootstrap support values (BP). Fully supported values are marked by an asterisk (*), and BP values below 80 are shown in gray. (B) Distribution of intra- and interspecific genetic distances among analyzed species based on the Kimura 2-parameter model for *COI* sequences. (C, D) The distribution information for each species. Circles represent collection localities, with numbers corresponding to localities of the sequence data in the phylogenetic tree.

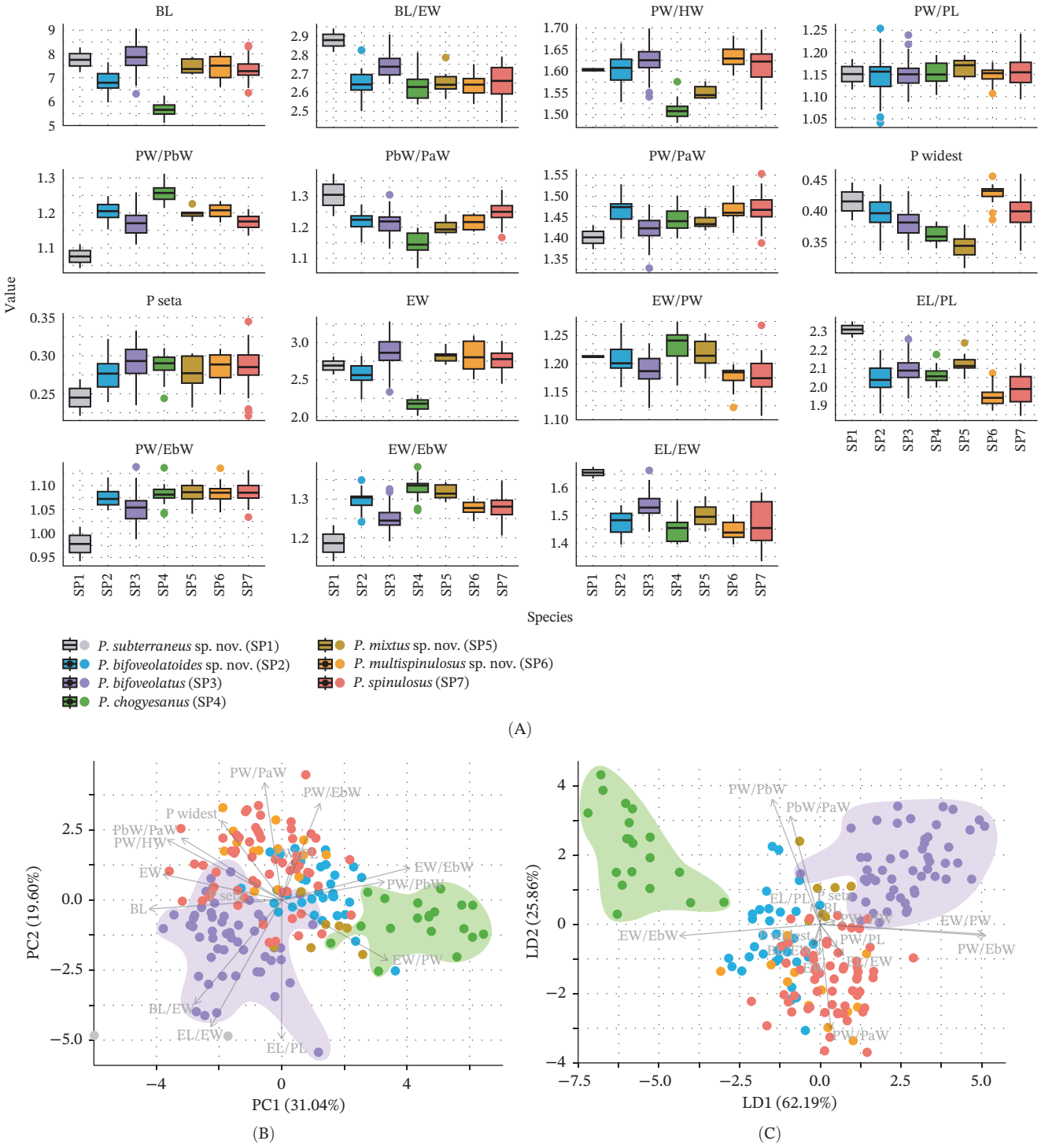

FIGURE 7 | (Continued)

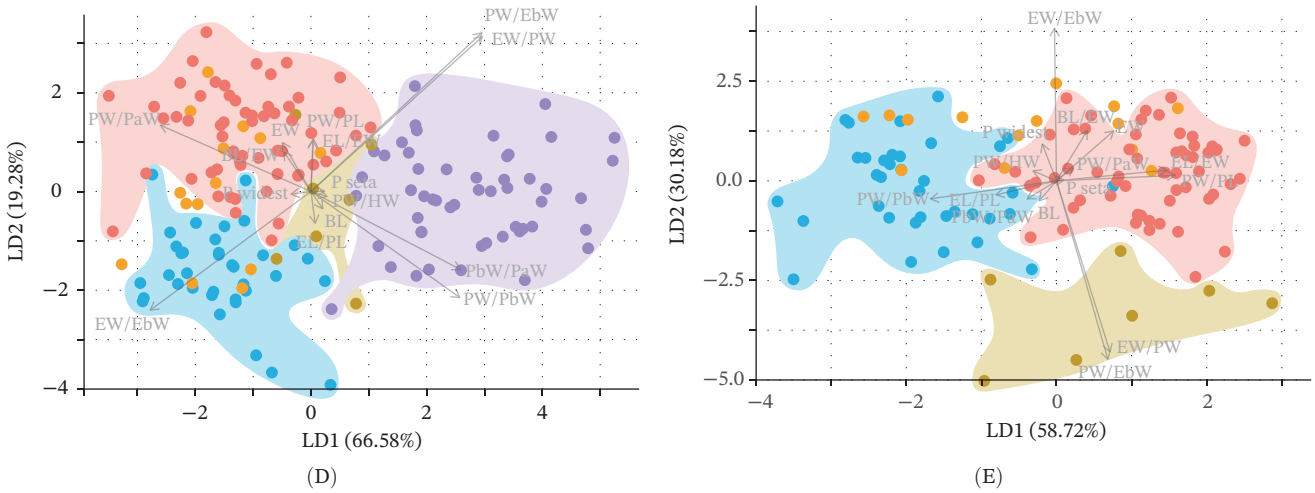

FIGURE 7 | Traditional morphometric analysis results of the Korean *Abea* species. (A) Boxplots of two raw measurements and 13 ratios. (B) PCA biplot based on seven species. (C) LDA biplot based on six species, excluding *P. subterraneus*. (D) LDA biplot based on five species, additionally excluding *P. chogyesanus*. (E) LDA biplot based on four species, additionally excluding *P. bifoveolatus*.

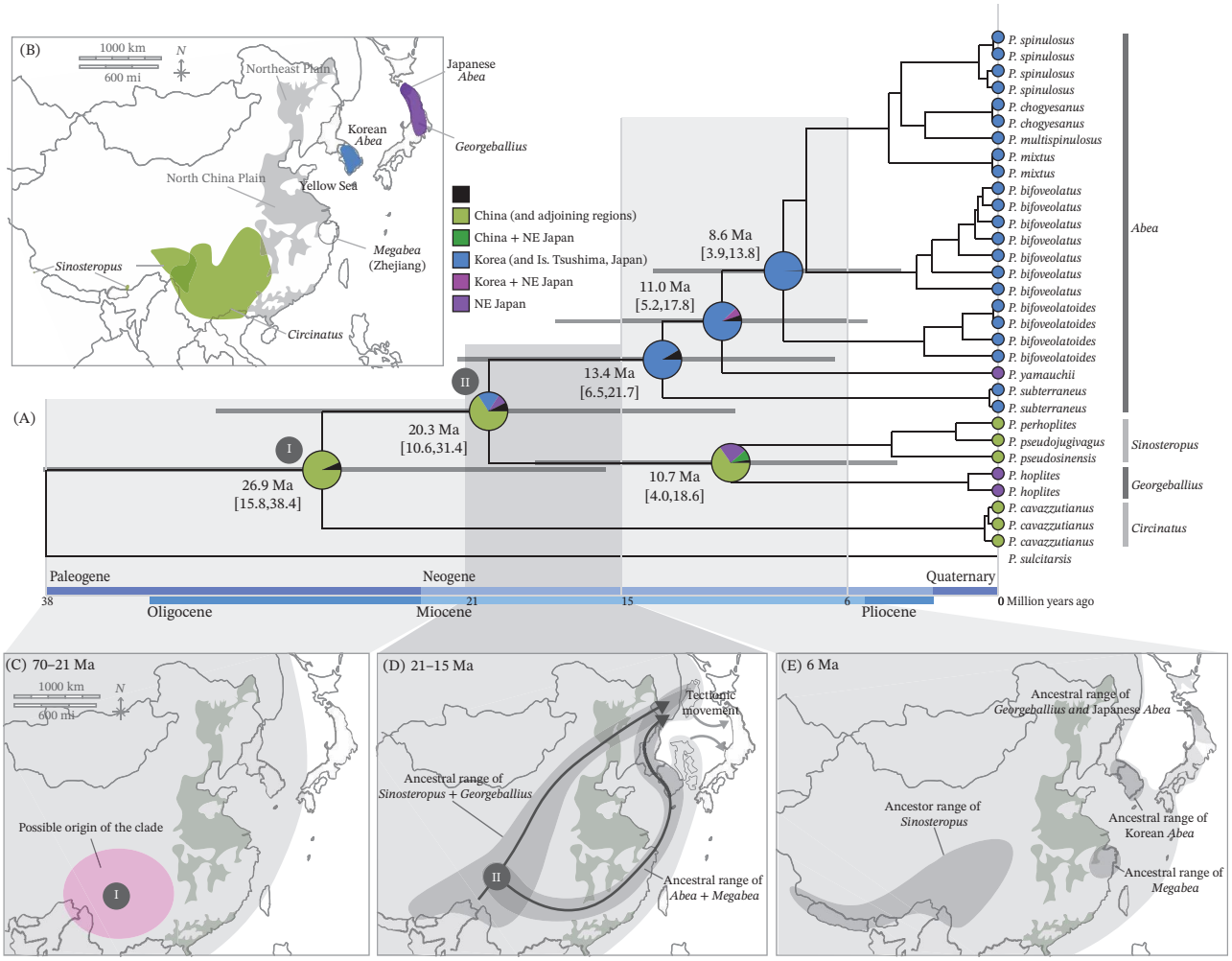

FIGURE 8 | Biogeographic hypothesis for *Abea* and related subgenera. (A) Results of the BEAST and RASP analyses for *Abea* and related subgenera. (B) Present distribution range of each subgenus. Gray shading indicates lowlands in eastern China, including the Northeast and North China Plains. (C–E) Proposed dispersal routes of *Abea* and its related subgenera. The paleomaps are based on previous studies [51–53]. Panel D illustrates tectonic movements near the Korean Peninsula from 21 to 15 Ma, following Otofuji et al. [51] and Tojo et al. [53]. Light gray shading indicates historically exposed landmasses (uncertain in southeastern China); pink shading marks a possible origin for the analyzed clade; and the dark gray area denotes the possible ancestral range of certain clades. The abbreviation 'NE' refers to the northeast.

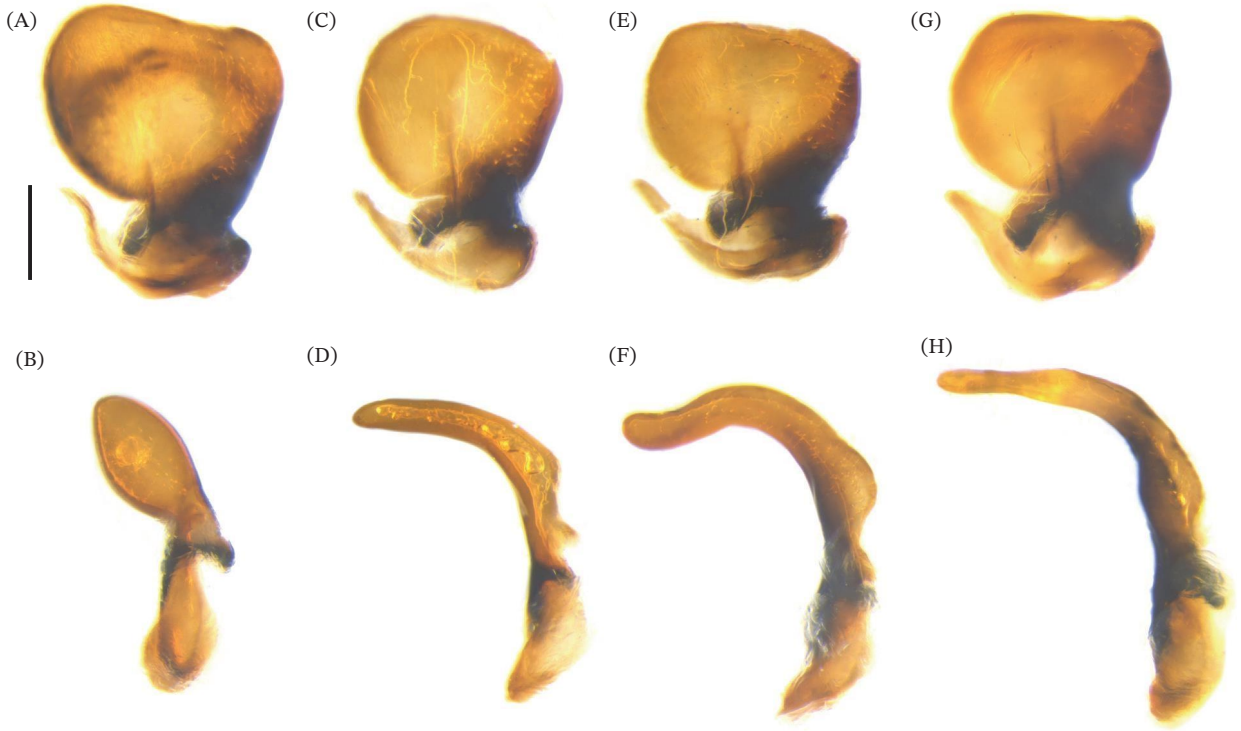

FIGURE 9 | Male genital parameres of four *Abea* species. Left parameres (A, C, E, G); right parameres (B, D, F, H). (A, B) *P. subterraneus* sp. nov. (C, D) *P. bifoveolatoides* sp. nov. (E, F) *P. mixtus* sp. nov. (G, H) *P. multispinulosus* sp. nov. Scale bar: 0.2 mm.

Ethira complex and *Nialoe* complex (sensu lato) was recovered, consistent with Schmidt et al. [6].

The ML tree of *Abea* and related subgenera (Figure 2B) strongly supported the synonymy of *Micronialoe* and *Abea*, as the latter was nested within the *Micronialoe* clade. The largest K2P distance between *Abea* and *Micronialoe* (3.0%) was smaller than the largest interspecific distance within *Micronialoe* (3.4%) (Table 1). Morphological examination corroborates this synonymy, as part of the *Micronialoe* species were also found to possess stout and linear right paramere (Figures 9B and 10K,L), which was previously considered the only character distinguishing between *Abea* and *Micronialoe* [2, 3]. Furthermore, the morphology of the right paramere is quite variable within some pterostichine subgenera (e.g., *Sinosteropus*, see Sciaky [54]; *Pseudohaptoderus*, see Facchini and Sciaky [55]; *Wraseiellus*, see Shi et al. [56]), making it an inadequate subgeneric diagnostic character. Following the taxonomic priority, *Micronialoe* becomes a junior synonym of *Abea*. *Abea* is differentiated from related subgenera by the absence of parascutellar striole, parascutellar pore, and setigerous pore on interval 3 of the elytra.

4.2 | Phylogenetic Relationships of Korean *Abea*

The phylogenetic analyses based on three datasets (Figures 2, 5, 6) consistently supported *P. subterraneus* sp. nov. as a sister to the remaining *Abea* species and close relationships between *P. spinulosus*, *P. multispinulosus* sp. nov., and *P. mixtus* sp. nov. However, interspecific relationships varied across datasets for the remaining species. One of the main controversies in interspecific relationships was the placement of *P. chogyesanus*. This species is unique in having features not present in other species: (i) the ostium of the median lobe of the aedeagus not turned to the left; (ii) the internal sac of the median lobe of the aedeagus with a single sclerotized part, which is the gonoporal piece. Current molecular and morphological data are vague to confirm its position. Besides, the relationship between *P. bifoveolatoides* sp. nov. and *P. bifoveolatus* was uncertain. Additional markers are needed for better resolution of the interspecific relationships within *Abea*.

4.3 | Species Delimitation of Korean *Abea*

Species classification based on male genital morphology identified eight distinct morphotypes (Table 2; Figure 5A). The phylogenetic analyses based on the *28S rRNA* (Figure 2B, Dataset 2) and concatenated datasets (Figure 5A, Dataset 3) supported the seven major clades. In contrast, the ML tree based on the *COI* dataset supported six clades by nesting *P. multispinulosus* within the clade of *P. spinulosus* (Figure 6A).

Among eight morphotypes, one male genital type (Morphotype 8) formed a clade with *P. spinulosus* in all phylogenetic analyses (Figures 2, 5, 6). It differs from the typical form by the location of the spiny patch in the median lobe of the aedeagus (Table 2; Figure 5A), which could now be regarded as an intraspecific variation. Even though *COI* data support *P. multispinulosus* within the *P. spinulosus* clade, genetic divergence of *28S rRNA* (1.7%–1.8%) and the difference in genital morphology (Table 2) support a clear separation of the species from the *P. spinulosus* clade members. In the case of two specimens of *P. subterraneus* from Mt. Juwangsan (GB) and Gwangjurigul Cave (CB), they exhibited 1.5% divergence

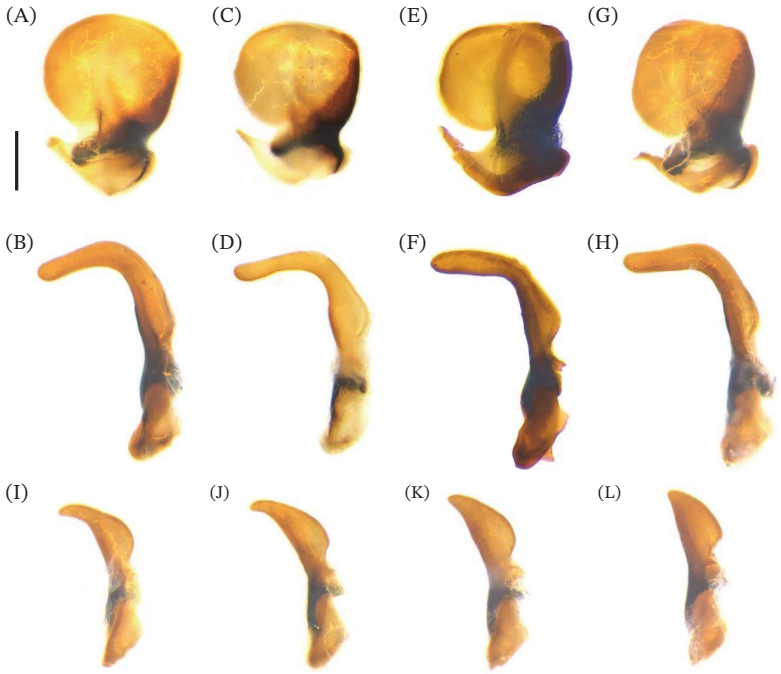

FIGURE 10 | Male genital parameres of three *Abea* species. Left parameres (A, C, E, G); right parameres (B, D, F, H, I–L). (A, B) *P. bifoveolatus* from the western part of Mt. Jirisan (JN). (C, D) Ditto from Mt. Wangsan (GN). (E, F) *P. spinulosus* from Mt. Hwasan (GB). (G, H) Ditto from Mt. Goheonsan (GN). (I, J) *P. chogyesanus* from the western part of Mt. Jirisan (JN). (K, L) Ditto from Mt. Baegunsan (JN). Scale bar: 0.2 mm.

in *COI* but were identical in *28S rRNA* sequences, supporting them as a single species. Overall, we recognize seven *Abea* species in Korea based on our current data.

Aside from the species pair of *P. multispinulosus* and *P. spinulosus*, the interspecific divergences of *COI* among the Korean *Abea* species were higher than 2.8%, which falls within the interspecific divergence range reported for German *Pterostichus* species, which was generally higher than 2.2% [9]. Compared to the *Hypherpes* complex [5], which is another flightless group within *Pterostichus*, Korean *Abea* species show relatively lower intraspecific divergence. In the *Hypherpes* complex, the intraspecific divergence reached up to 2.3% for *28S rRNA* and 3.1% for *COI* (vs., 0.9% and 1.5% in *Abea*). This could imply that the Korean *Abea* species may have undergone a relatively recent population expansion compared to the Nearctic *Hypherpes* complex.

4.4 | Morphometric Analyses

In our morphometric results (Figure 7), *P. subterraneus* and *P. chogyesanus* showed potential for separation from other species. However, the remaining species were not clearly distinguishable, since most of the measured ratios exhibited broad ranges, making it difficult to delineate species boundaries solely based on morphometric data. This finding highlights the limited resolution of morphometric data alone and implies the importance of male genital characters and molecular markers for accurate species identification. It poses a significant challenge for the morphological identification of female specimens, as they lack diagnostic genital characters.

4.5 | Morphological Evolution of *Abea*

The consistent recovery of monophyletic subterranean (*P. subterraneus*) and epigean clades (the remaining species) within the genus *Abea* across analyses (Figures 2, 5, 6) suggests ecological niche differentiation as a driver of primary divergence. The subterranean clade exhibits classic troglomorphic traits, including reduced eyes and depigmentation (Figures 11A,B and 12A), indicative of adaptation to hypogean environments. Furthermore, numerous setae are found on the pit of the mentum for *P. subterraneus*, while those are not observable in the epigean clade.

A potential case of convergent evolution was identified in the *P. bifoveolatus* specimen from Mt. Wangsan. A single male specimen was collected at a shallow depth, under stacked fist-sized rocks. It exhibits troglomorphic traits such as smaller eyes and lighter coloration compared to the remaining conspecific specimens (Figure 13C). It also shares the following characters with *P. subterraneus*: (i) pronotal anterior angle sharp and distinctly protruded (Figure 14E); (ii) elytra narrow and elongate (Figure 13C). Similar morphological adaptations are observed in other *Pterostichus* subgenera, such as *Licentius* and *Qianius* (see Jia et al. [57]), as well as outside of the genus, such as the genera *Abacaecus* of the tribe Abacetini (see Allegro and Giachino [58]) and *Jujiroa* of the tribe Platynini (see Habu [59] and Morita [60]), suggesting the possibility of convergent evolution under similar environmental pressures in subterranean habitats.

Our results also provide insights into the male genital evolution within the Korean *Abea* species (Figure 5A). The most recent common ancestor of the clade is highly likely to have possessed

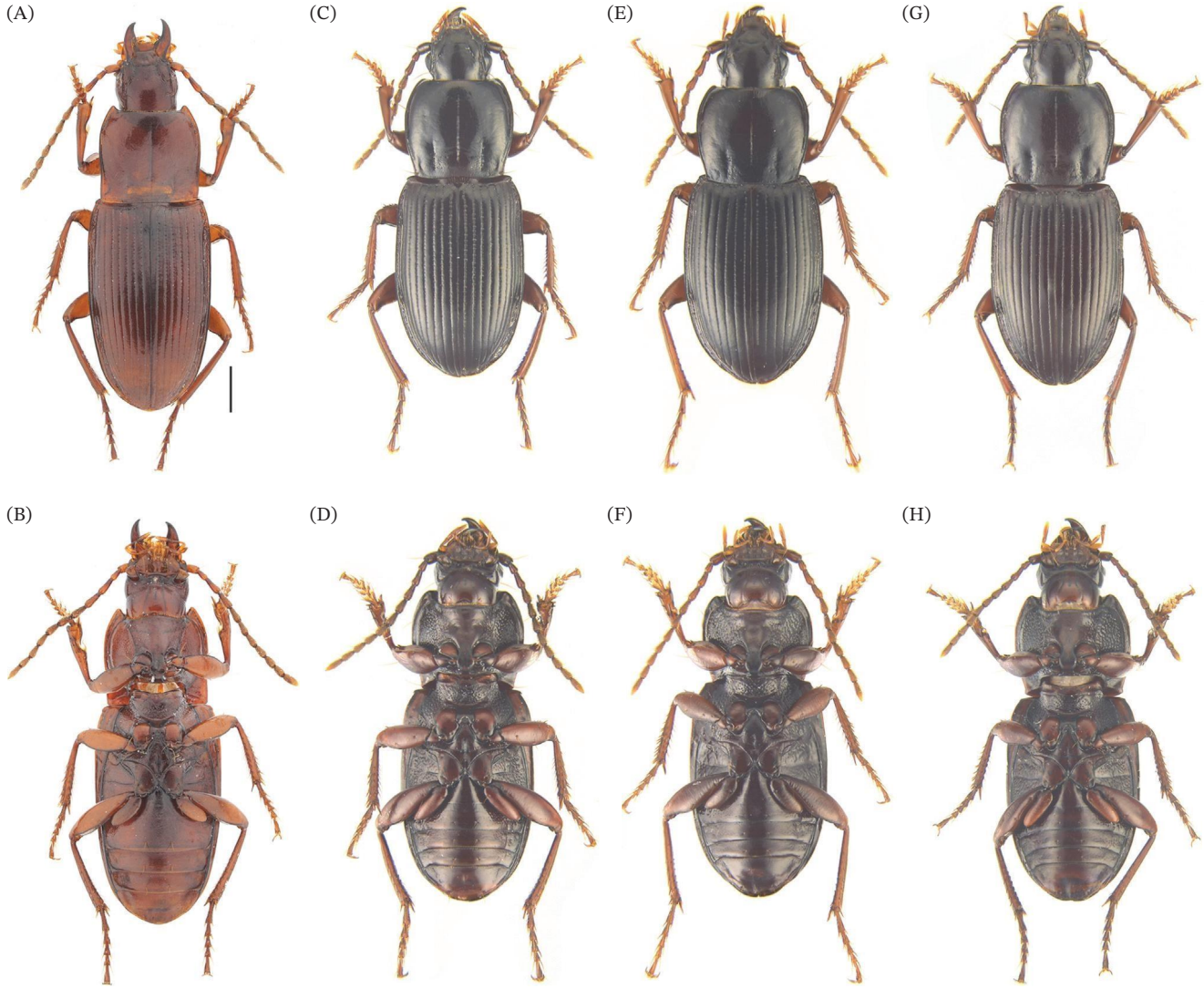

FIGURE 11 | Habitus of four *Abea* species. (A, B) *P. subterraneus* sp. nov. (C, D) *P. bifoveolatoides* sp. nov. (E, F) *P. mixtus* sp. nov. (G, H) *P. multispinulosus* sp. nov. Dorsal view (A, C, E, G) and ventral view (B, D, F, H). Scale bar: 1 mm.

two sclerotized pieces in the internal sac of the male genitalia, including the gonoporal piece and the ventral sclerite, as the early diverging species have this trait. The loss of the ventral sclerite may have occurred only in the clade of *P. chogyesanus*. The species with a spiny patch formed a monophyletic clade in the ML analyses of both concatenated and *COI* datasets (Figures 5A and 6A), suggesting a single evolutionary origin of this character. On the other hand, the species with the carina on the median lobe of the aedeagus did not form a monophyletic clade, indicating repeated independent evolution.

4.6 | Perspectives on the Biogeographical History of *Abea* and Relatives

4.6.1 | Dispersal and Distribution Expansion From China to Korea

The time-calibrated phylogenetic and RASP analyses (Figure 8) suggested that the southern part of China, where *Circinatus* and *Sinosteropus* are distributed, may represent the ancestral area of the clade (Figure 8C). We hypothesize that ancestral *Abea* dispersed from the southern part of China, via Zhejiang, to Korea and Japan (Figure 8D). This scenario is based on the presence of the subgenus *Megabea* in Zhejiang, China ([61]; Figure 8B), a possible close relative of the Korean *Abea* species based on morphological features [2].

A parallel example is found in East Asian *Hynobius* salamanders, where phylogeographic analysis revealed close relationships between the southeastern Chinese and the southwestern Japanese clade [62]. This suggests a possible dispersal route through the Fukien-Reinan massif, which connected these regions during the late Oligocene and early Miocene. Given that *Abea* diverged from *Sinosteropus* + *Georgeballius* in the early Miocene, dispersal along the Fukien-Reinan massif is chronologically plausible. Geological continuity between southeastern China and southern Korea [63] lends additional support.

This hypothesis, however, remains tentative due to potential barriers. First, paleo-river systems in eastern China may have hindered dispersal. Although the Yellow Sea between China and the Korean Peninsula (Figure 8C–E) was possibly part of the continent until ~2.0 Ma [52], some paleo-river systems likely drained toward the

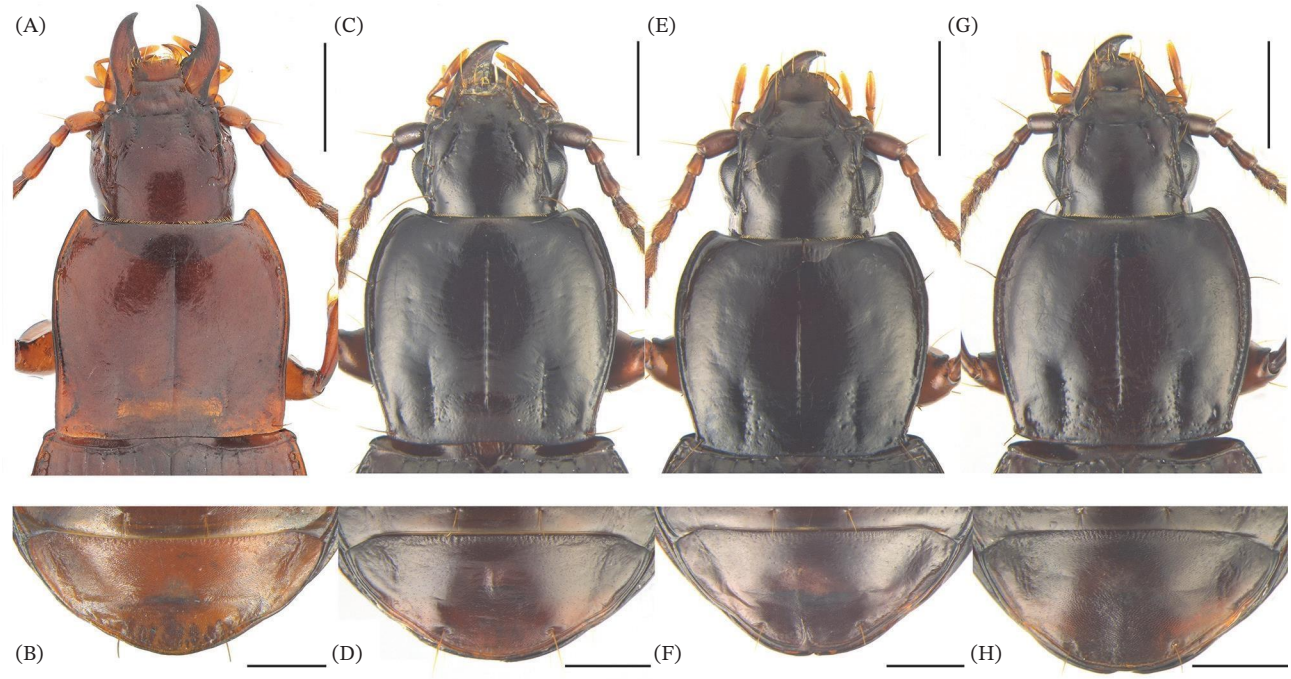

FIGURE 12 | Head, Pronotum (A, C, E, G), and male last abdominal sternite (B, D, F, H) of four *Abea* species. (A, B) *P. subterraneus* sp. nov. (C, D) *P. bifoveolatoides* sp. nov. (E, F) *P. mixtus* sp. nov. (G, H) *P. multispinulosus* sp. nov. Dorsal view (A, C, E, G) and ventral view (B, D, F, H). Scale bars: 1 mm (A, C, E, G); 0.5 mm (B, D, F, H).

continental margin, separating southeastern China from Korea and Japan. For example, the paleo-Yellow River system may have flowed between the Korean Peninsula and southeast China since 50–40 Ma [64]. Such systems could have served as barriers to the dispersal of small, flightless carabid beetles. Second, climatic heterogeneity along the longitudinal axis of the proposed route may also have constrained dispersal.

An alternative hypothesis involves dispersal along the mountain ranges extending from southern to northeastern China (the route for *Sinosteropus* + *Georgeballius* in Figure 8D). While this route also involves a south-to-north movement, the similar climatic conditions along a certain altitudinal range may have facilitated dispersal through mountain ranges. Additionally, this pathway avoids the major lowland regions that may have posed ecological barriers.

4.6.2 | Dispersal to Northeast Japan

In Japan, *Abea* and *Georgeballius* are known to be distributed in the northeastern part of Honshu [1, 4, 40, 42]. We suggest that these taxa diverged during the tectonic movement around 21–15 Ma in East Asia (Figure 8D, E), a key geological period facilitating the dispersal and divergence of terrestrial taxa between the continent and the Japanese Archipelago (e.g., [53, 62]). During this period, the landmass near the southern part of the Korean Peninsula rotated clockwise, forming southwestern Japan, and the landmass near the Far East rotated anticlockwise, forming northeastern Japan [51]. Divergence of these Japanese taxa from their relatives is estimated to be late Miocene, around 11 Ma (Figure 8A), slightly younger than the period of the tectonic movement. However, the absence of these groups from the southwestern part of Japan could suggest a low possibility of dispersal from the south. Although *Georgeballius* was recorded from Kyushu by Bates [65], no subsequent confirmations have been identified thereafter. The discrepancy in timing may reflect limited molecular sampling or uncertainties in calibration.

Pterostichine diversity across China and neighboring regions is extraordinarily rich and actively studied (e.g., [2, 41, 56, 57, 61, 66–70]). Expanding molecular datasets of supraspecific taxa from China and related regions will elucidate interesting historical dispersal patterns of the genus *Pterostichus* across East Asia.

4.7 | Taxonomic Account

Family Carabidae Latreille, 1802

Tribe Pterostichini Sloane, 1920

Subtribe Pterostichina Sloane, 1920

Genus *Pterostichus* Bonelli, 1810

4.7.1 | Subgenus *Abea* Morita, 1992

Abea Morita (1992) [1]:15. Type species: *Pterostichus yamauchii* Morita, 1992.

Micronialoe Park, Kwon & Lafer, 1996 [71]:73. Type species: *Pterostichus bifoveolatus* Park, Kwon & Lafer, 1996. Synonymy designated in this study.

Diagnosis. Besides the following, refer to Kim and Suh [2]: body color reddish brown to black. Eyes moderate-sized to almost reduced; supraorbital pores rarely three pairs. Right paramere of male genitalia stout or slender and curved.

Redescription. See Kim and Suh [2].

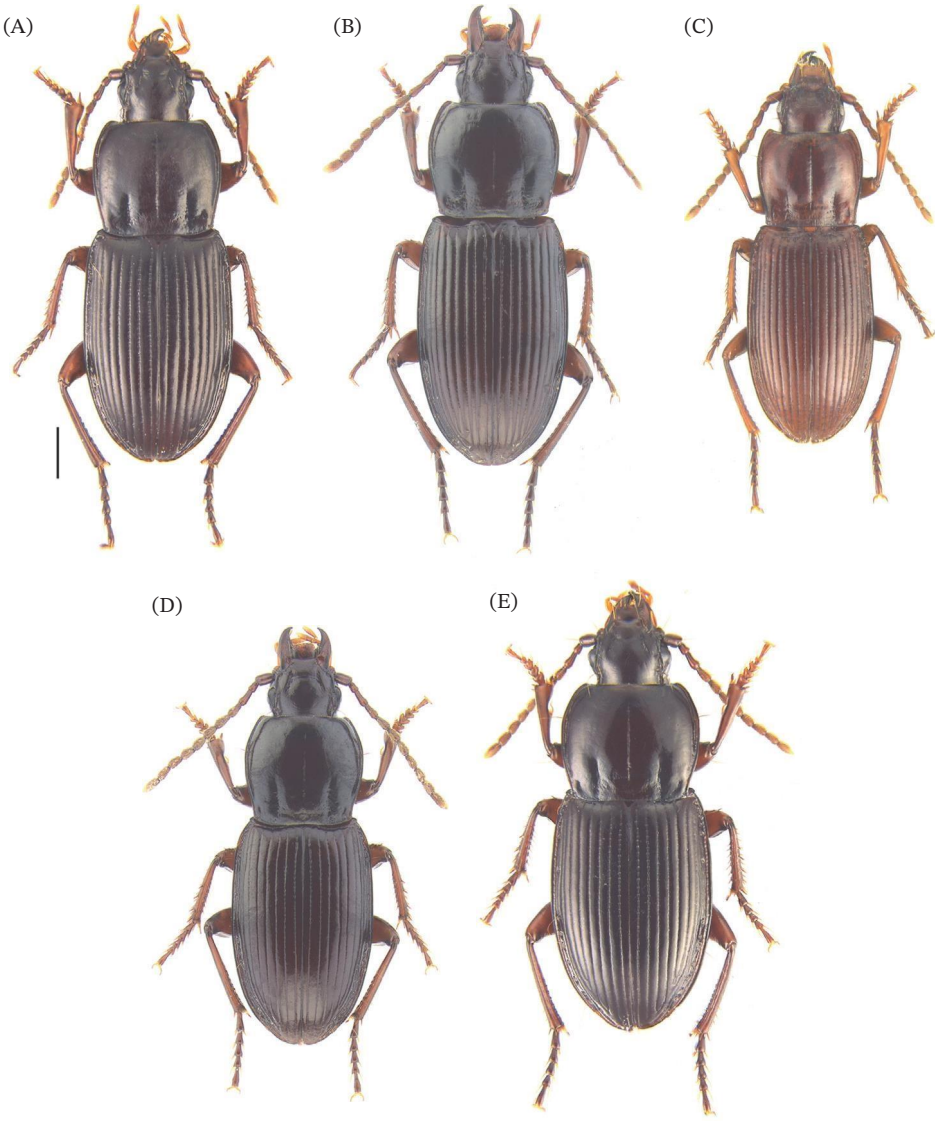

FIGURE 13 | Dorsal habitus of two *Abea* species. (A) *P. bifoveolatus* from the western part of Mt. Jirisan (JN). (B) Ditto from Mt. Choejeongsan (DG). (C) Ditto from Mt. Wangsan (GN). (D) *P. spinulosus* from Mt. Hwasan (GB). (E) Ditto from Mt. Goheonsan (GN). Scale bar: 1 mm.

Remarks. *Megabea* Sciaky also seems to be a junior synonym of *Abea*.

Ecology. The members of the subgenus usually dwell in the forest. In Korea, most of the individuals were collected under rocks near the mountain valley. Sometimes, they were also found below ground or under the bark of the rotten tree.

4.7.2 | *Pterostichus* (*Abea*) *subterraneus* Kim, Seo & Hwang sp. nov.

(Figures 1B, 3A-E, 9A,B, 11A,B and 12A,B,)

urn:lsid:zoobank.org:act:F50027C3-682A-4DA0-BA9F-534961F4763B

Korean name: 지하꼬마길쭉먼지벌레 [신칭]

Type specimens. *Holotype*: 1♂; GB, Cheongsong-gun, Juwangsan-myeon, Sangui-ri, Mt. Juwangsan; alt. ca 380 m; 36°24′12.8″N 129°10′18.1″E; 3.V.2023; Jangwon Seo; Project coll. NIBR202304105 (Vial & DNA Voucher No. JWMicro1). *Paratype*: 1♀; CB, Okcheon-gun, Cheongseong-myeon, Jangsu-ri, Gwangjurigul Cave; alt. ca 220 m; 36°17′59.5″N 127°44′12.3″E; 6.VI.2023; Jangwon Seo (Vial & DNA Voucher No.: GJRCMicro1).

Diagnosis. This new species is the most peculiar among its consubgeners by having a light body color, almost reduced eyes, and additional setae near a pair of pits in the mentum (Figure 11A,B). Other significant characters are as follows.

Pronotum (Figure 12A) with two pairs of basal foveae; inner fovea shallow and outer fovea almost invisible. Posteromedian area of male sternite VII (Figure 12B) with one distinctly transverse ridge slightly behind middle, microsculpture consisting of irregular transverse polygonal meshes. Median lobe of aedeagus (Figure 3A–E) slender; apex narrowly rounded in dorsal view, deeply emarginate in right lateral side; ventral carina absent; sclerotized areas of internal sac consist of the following: (i) gonopore piece on median area; (ii) moderate sized, triangular-shaped ventral sclerite on subapical area; right

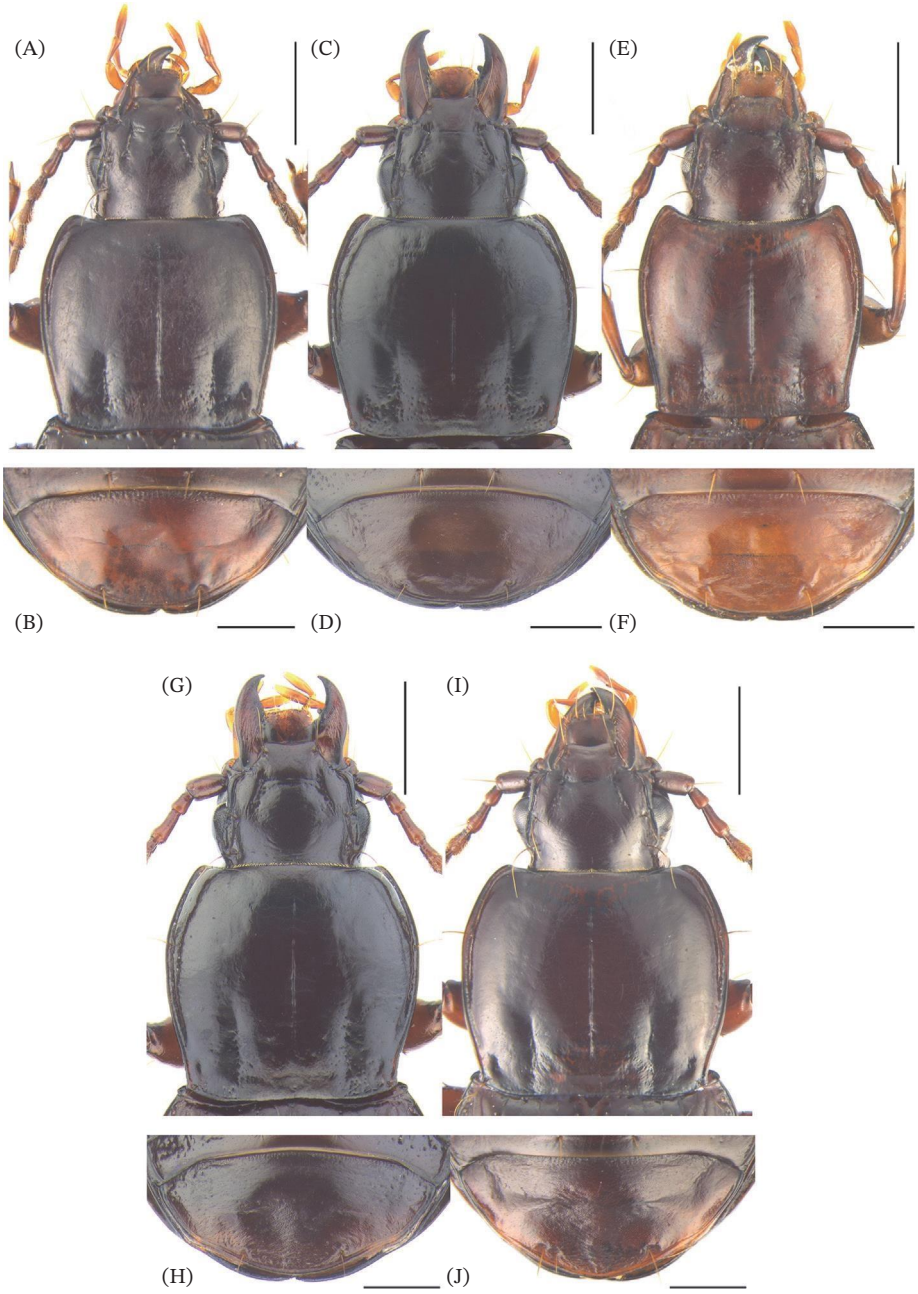

FIGURE 14 | Head, Pronotum (A, C, E, G, I), and male last abdominal sternite (B, D, F, H, J) of two *Abea* species. (A, B) *P. bifoveolatus* from the western part of Mt. Jirisan (JN). (C, D) Ditto from Mt. Choejeongsan (DG). (E, F) Ditto from Mt. Wangsan (GN). (G, H) *P. spinulosus* from Mt. Hwasan (GB). (I, J) Ditto from Mt. Goheonsan (GN). Dorsal view (A, C, E, G, I) and ventral view (B, D, F, H, J). Scale bars: 1 mm (A, C, E, G, I); 0.5 mm (B, D, F, H, J).

paramere (Figure 9B) stout, distinctly curved near middle, swollen before apex.

Description. Body length: 7.2–8.3 mm, width: 2.6–2.8 mm.

Coloration (Figure 11A, B). Reddish brown and shiny; margin of mandible, joints between femur and tibia darker; palpi yellowish brown, with apices distinctly paler; ventral side reddish brown.

Head (Figure 12A). Eye almost reduced; tempus developed, widely convex; frontal impression shallow, tilted toward anterior supraorbital pore; supraorbital pores consisting of two (holotype, HT) or three (paratype, PT) pairs; mentum with additional setae near a pair of pits.

Pronotum (Figure 12A) widest near 2/5 from apex; apical angle narrowly rounded, distinctly protruded anteriorly; lateral margin weakly convex anteriorly, faintly sinuate before basal angle; anterolateral seta before widest point, near 1/4 from apex; basal angle slightly obtuse, not protruded laterally; anterior transverse impression faint or absent; posterior transverse impression shallow; inner basal foveae shallow, linear, almost parallel, with punctures basally; outer foveae almost invisible; area between inner foveae weakly rugose transversely; area between inner fovea and outer fovea almost glabrous. PW/HW = 1.60 (HT), 1.61 (PT); PW/PL = 1.12 (HT), 1.19 (PT); PW/PbW = 1.04 (HT), 1.11 (PT); PW/PaW = 1.43 (HT), 1.37 (PT); PbW/PaW = 1.37 (HT), 1.24 (PT).

Elytra widest before or behind middle; striae shallow basally, laterally, and apically, punctate from base to basal half; marginal umbilicate series composed of three groups, humeral group with 5 pores, medial group with one pore, and apical group with six pores. EW/PW = 1.21 (HT), 1.22 (PT); EL/PL = 2.27 (HT), 2.35 (PT); EL/EW = 1.68 (HT), 1.64 (PT).

Ventral side (Figures 11B and 12B). Posteromedian area of male sternite VII with one distinctly transverse ridge slightly behind middle, microsculpture consisting of irregular transverse polygonal meshes (Figure 12B).

Male genitalia (Figures 3A–E, 9A,B). Median lobe of aedeagus (Figure 3A–E) slender, well curved in lateral view, almost linear in dorsal view; ventral side distinctly curved near middle, and almost linear apically; left lateral margin below apical orifice faintly convex; apical orifice bent to left; terminal lamella very short; apex narrowly rounded in dorsal view, deeply emarginate in right lateral side; ventral carina absent; internal sac with two sclerotized areas: (i) gonopore piece on median area and (ii) moderate sized, triangular-shaped ventral sclerite on subapical area; left paramere (Figure 9A) widens toward apex; right paramere (Figure 9B) stout, distinctly curved near middle, swollen before apex.

Type locality. Mt. Juwangsan, Cheongsong-gun, S. Korea (Figure 1B).

Distribution. See Figure 1B.

Etymology. The specific name "*subterraneus*" refers to the ecological characteristic of the new species.

Ecology. The holotype specimen was observed at a depth of 50 cm beneath the surface, and the paratype specimen was collected in the deepest chamber of the Gwangjurigul cave.

Variations. Even though a significant difference was identified in the number of supraorbital pores between the holotype and paratype, we consider these to be conspecific based on our pairwise genetic distance analyses in the *28S rRNA* sequence (0.0%; Table 1). Additionally, three pairs of the supraorbital pores have not been found in other *Abea* specimens; therefore, the paratype specimen may be in an abnormal form or could be a feature of the population within the Gwangjurigul Cave. The male specimen from this cave must be examined in the future to clarify its taxonomic status.

Remarks. This species is the first subterranean-adapted *Pterostichus* species from the Korean Peninsula.

4.7.3 | *Pterostichus* (*Abea*) *bifoveolatoides* Kim & Hwang sp. nov.

(Figures 1B, 3F–J, 9C,D 11C,D and 12C,D)

urn:lsid:zoobank.org:act:602F9D87-17E2-4E44-B612-24D00561471A

Korean name: 닮음꼬마길쭉먼지벌레 [신칭]

Type specimens. *Holotype*: 1♂; GB, Andong-si, Dosan-myeon, Dancheon-ri, near Mt. Cheongryangsan; alt. ca 600 m; 36°44′55.0″N 128°54′53.3″E; 31.VIII.2023; Dooyoung Kim (Vial & DNA Voucher No. CRMicro1). *Paratypes*: GB – 1♂; GB, Yecheon-si, Hyoja-myeon, Gohang-ri, near Mt. Sobaeksan; alt. ca 560 m; 36°50′14.0″N 128°27′39.1″E; 27.VII.2021; Dooyoung Kim (Vial No. SBMicro1). 1♂; GB, Yeongyang-gun, Seokbo-myeon, Simui-ri, Mt. Podosan; alt. ca 490 m; 36°31′05.7″N 129°13′00.4″E; 6. VI.2023; Dooyoung Kim (Vial & DNA Voucher No. YYMicro1). 4♂2♀; same data as for holotype (Vial No. CRMicro2–5). 1♂; GB, Pohang-si, Buk-gu, Gibuk-myeon, Tapjeong-ri, Mt. Bihaksan; alt. ca 390 m; 36°08′47.6″N 129°13′09.8″E; 22.VII.2023; Dooyoung Kim (Vial & DNA Voucher No. PHMicro1). 1♂; GB, Uljin-gun, Maehwa-myeon, Gilgok-ri; 36°47′46.9″N 129°19′19.8″E; 21. VI.2024; Geonhyeok Kim, Yongtae Jang (Vial No. UJMicro1). GG – 3♂3♀; GG, Gapyeong-gun, Gapyeong-eup, Dumil-ri, Gitdaebong Peak; alt. ca 490 m; 37°50′02.2″N 127°25′24.1″E; 12.VIII.2023; Dooyoung Kim (Vial No. GPMicro1–4). GW – 1♂; GW, Wonju-si, Panbu-myeon, Seogok-ri, Mt. Baegunsan; alt. ca 640 m; 37°15′40.5″N 127°57′48.2″E; 4.VI.2023; Dooyoung Kim (Vial & DNA Voucher No. WJMicro1). 2♂1♀; GW, Pyeongchang-gun, Yongpyeong-myeon, Nodong-ri, near Mt. Gyebangsan; alt. ca 850 m; 37°41′43.1″N 128°28′42.7″E; 9.VI.2023; Dooyoung Kim (Vial No. GBMicro1, 2; DNA Voucher No. GBMicro1). 1♂; GW, Pyeongchang-gun, Jinbu-myeon, Jangjeon-ri, Mt. Gariwangsan; alt. ca 920 m; 37°27′56.2″N 128°32′15.9″E; 9.VI.2023; Dooyoung Kim (Vial & DNA Voucher No. GRWMicro1). 1♂1♀; GW, Inje-gun, Inje-eup, Gosa-ri, Mt. Hanseoksan; alt. ca 520 m; 38°03′17.2″N 128°12′50.9″E; 7. VIII.2024; Dooyoung Kim, Hyejeong Yu (Vial No. HSSMicro1). 1♂1♀; GW, Inje-gun, Inje-eup, Gwidun-ri, Mt. Jeombongsan; alt. ca 940 m; 38°01′23.0″N 128°25′53.8″E; 8.VIII.2024; Dooyoung Kim, Hyejeong Yu (Vial No. JBMicro1). CB – 5♂2♀; CB, Yeongdong-gun, Sangchon-myeon, Mulhan-ri, Mt. Minjujisan; alt. ca 720 m; 36°03′01.9″N 127°51′58.0″E; 1.VII.2023; Dooyoung Kim (Vial No. MJJMicro1–5; DNA Voucher No. MJJMicro1). CN – 1♂1♀; CN, Gongju-si, Sinpung-myeon, Ssangdae-ri; alt. ca 160 m; 36°28′13.8″N 126°55′30.2″E; 18.VI.2023; Dooyoung Kim (Vial No. GJMicro1, 2; DNA Voucher No. GJMicro1).

Other specimens examined. 1♀; GB, Mungyeong-si; Maseong-myeon, Oeeo-ri, Mt. Seonamsan; alt. ca 470 m; 36°41′34.6″N 128°10′30.5″E; 7. V.2023; Dooyoung Kim (Vial No. MGMicro1). 1♀; CB, Geumsan-gun, Chubu-myeon, Yogwang-ri, Gulgol Valley; alt. ca 260 m; 36°13′16.8″N 127°28′38.8″E; 18.VI.2023; Dooyoung Kim (Vial No. GESMicro1).

Diagnosis. The new species is very similar to *P. bifoveolatus* and can be best distinguished from it by male characters. The most important character state that sets the new species apart from *P. bifoveolatus* is its absence of the carina in the median lobe of the aedeagus (Figure 3G). Also, the longitudinal ridge on the anteromedian area of the male sternite VII (Figure 12D) is hitherto unique to this species compared to consubgeners. Other significant characters are as follows.

Pronotum (Figure 12C) with two pairs of basal foveae; outer fovea sometimes absent. Median lobe of aedeagus (Figure 3F–J) stout; apex narrowly rounded; sclerotized areas of internal sac consist of the following: (i) gonopore piece on median area; (ii) oval-shaped ventral sclerite on subapical area.

Description. Body length: 6.0–7.6 mm, width: 2.2–2.8 mm.

Coloration (Figure 11C, D) black or brownish black and shiny; antennae, legs, and lateral margin of pronotum and elytra dark

brown; palpi yellowish brown, with apices distinctly paler; ventral side overall black, sternites brownish black.

Head (Figure 12C). Eye moderately convex; tempus developed, weakly convex; frontal impression deep, tilted toward anterior supraorbital pore.

Pronotum (Figure 12C) widest around 2/5 from apex; apical angle narrowly rounded, slightly protruded anteriorly; lateral margin faintly to distinctly sinuate, rarely fully convex; anterolateral seta before widest point, near 1/4 to 3/10 from apex; basal angle slightly obtuse, slightly or not protruded laterally; anterior and posterior transverse impression faint or absent; inner basal foveae deep, linear, almost parallel, frequently with faint to distinct punctures; outer foveae generally distinct, but almost invisible in some specimens; area between inner foveae with or without shallow punctures, rarely distinct, and frequently with short transverse rugosus along basal margin; area between inner fovea and outer fovea almost glabrous. PW/HW = 1.53–1.67, mean 1.60; PW/PL = 1.04–1.25, mean 1.15; PW/PbW = 1.15–1.25, mean 1.20; PW/PaW = 1.40–1.53, mean 1.47; PbW/PaW = 1.15–1.27, mean 1.22 in 24 males and 12 females.

Elytra widest in or behind middle; striae shallow basally, laterally, and apically, slightly deeper medially, punctures distinct from base to basal half; marginal umbilicate series composed of three groups, humeral group with five pores, medial group with one pore, and apical group with seven pores (rarely six or eight pores). EW/PW = 1.16–1.27, mean 1.21; EL/PL = 1.86–2.20, mean 2.04; EL/EW = 1.39–1.54, mean 1.47 in 24 males and 12 females.

Ventral side (Figures 11D and 12D). Posteromedian area of male sternite VII depressed, flat, longitudinal ridge in anteromedian part, with microsculpture consisting of irregular wide transverse meshes (Figure 12D).

Male genitalia (Figures 3F–J and 9C,D). Median lobe of aedeagus (Figure 3F–J) stout, well curved in lateral view, almost linear in dorsal view; ventral side distinctly curved behind basal bulb and gently curved toward apex; left lateral margin below apical orifice slightly convex; apical orifice bent to left; terminal lamella very short; apex narrowly rounded in dorsal view; ventral carina absent; internal sac with two sclerotized areas: (i) gonopore piece on median area, and (ii) moderate sized, oval-shaped ventral sclerite on subapical area; left paramere (Figure 9C) wide, rounded throughout apically; right paramere (Figure 9D) slender, distinctly curved, forming obtuse angle.

Type locality. Mt. Cheongryangsan, Andong-si, S. Korea (Figure 1B).

Distribution. See Figure 1B.

Etymology. The specific name "*bifoveolatoides*" refers to the similarity of the new species with *P. bifoveolatus*.

Ecology. This species was never found sympatrically with other species, though *P. subterraneus* is distributed within its distribution range.

Variations. Through examination of male specimens from 13 localities, we identified several variations in important characters. *Outer fovea of pronotum*: It is generally present, sometimes quite long. The individuals from Gongju-si (CN), Mt. Jeombongsan (GW), and Mt. Hanseoksan (GW) have a nearly reduced outer fovea. *Male sternite VII*: A short longitudinal ridge in the anteromedian part of the male sternite VII was consistently identified in all male specimens. However, its length, degree of elevation, and angle varied among populations. Individuals from Mt. Gyebangsan (GW), Mt. Baegunsan (GW), and Mt. Minjujisan (CB) had a very weakly elevated longitudinal ridge, almost superficial. One individual from Mt. Gyebangsan had an oblique ridge. *Male genitalia*: In the median lobe of the aedeagus, the carina was always absent, and no distinct variation was observed in the position of the gonopore piece. The shape of the ventral sclerite was generally similar in size but showed slight differences among populations. The most prevalent type was oval shape, as in Figure 3I, gradually narrowing apically. The population from Gapyeong-gun (GG) had quite a characteristic ventral sclerite, with the right side expanded and narrowly rounded. From the lateral view, there was variation in curviness. The specimens from Gapyeong-gun were more curved than those from the type locality.

4.7.4 | *Pterostichus* (*Abea*) *mixtus* Kim & Hwang sp. nov.

(Figures 1C, 3K–O, 9E,F, 11E,F, and 12E,F)

urn:lsid:zoobank.org:act:B937954D-B7CD-4512-9D06-787ACE294C66

Korean name: 중꼬마길쭉먼지벌레 [신칭]

Type specimens. *Holotype*: 1♂; JN, Damyang-gun, Weolsan-myeon, Yongheung-ri, Mt. Yonggusan; alt. ca 370 m; 35°20′12.9″ N 126°53′40.7″E; 24.IX.2023; Dooyoung Kim (Vial & DNA Voucher No. DYMicro1). *Paratype*: 1♀; JN, Hwasun-gun, Baega-myeon, Songdan-ri, Mt. Baegasan; alt. ca 480 m; 35°10′4.8″N 127°11′10.3″E; 24.IX.2023; Dooyoung Kim (Vial No. HSUMicro2). 1♀; same data as for preceding; 6.VII.2024; Dooyoung Kim (Vial & DNA Voucher No. HSUMicro1). 1♂; same data as for preceding; 31.V.2025; Dooyoung Kim, Hyejeong Yu (Vial No. HSUMicro3). 2♂1♀; same data as for holotype; 31.V.2025; Dooyoung Kim, Hyejeong Yu (Vial No. DYMicro2, 3).

Diagnosis. This species can be confidently identified through the apical border of the male abdominal sternite VII (Figure 12F), which sharply intrudes toward the medial part of the sternite. Other significant characters are as follows.

Pronotum (Figure 12E) with two pairs of basal foveae; inner foveae distinct and outer fovea superficial. Median lobe of aedeagus (Figure 3K–O) stout; apex almost truncate; ventral carina distinct; sclerotized areas of internal sac consist of the following: (i) gonopore piece on median area; (ii) moderate sized, water drop-shaped ventral sclerite on subapical area; and (iii) spiny patch consisting of numerous sclerotized, compact spines on subapical area.

Description. Body length: 7.1–7.9 mm, width: 2.7–3.0 mm.

Coloration (Figure 11E, F) black and shiny; antennae, legs, and lateral margin of pronotum and elytra dark brown; palpi yellowish brown, with apices distinctly paler; ventral side overall black, sternites brownish black.

Head (Figure 12E). Eye moderately convex; tempus developed, faintly convex; frontal impression deep, tilted toward anterior supraorbital pore.

Pronotum (Figure 12E) widest on 3/10 to 2/5 from apex; apical angle narrowly rounded, slightly protruded anteriorly; lateral margin convex throughout or faintly sinuate before basal angle; anterolateral seta before widest point, near 1/4 to 3/10 from apex; basal angle obtuse, faintly protruded laterally or not; anterior transverse impression faint; posterior transverse impression shallow or absent; inner basal foveae deep, linear, almost parallel, with punctures; outer foveae superficial; area between inner foveae punctate only near the foveae, sometimes distinctly rugose transversely; area between inner fovea and outer fovea almost impunctate or with very weak punctures. PW/HW = 1.54–1.58, mean 1.55; PW/PL = 1.14–1.19, mean 1.17; PW/PbW = 1.18–1.23, mean 1.20; PW/PaW = 1.42–1.47, mean 1.44; PbW/PaW = 1.18–1.24, mean 1.20 in four males and three females.

Elytra widest near or behind middle; striae shallow basally, laterally, and apically, slightly deeper medially, punctures distinct from base to basal half; marginal umbilicate series composed of three groups, humeral group with five pores (rarely six), medial group with one pore, and apical group with seven or eight pores. EW/PW = 1.17–1.25, mean 1.22; EL/PL = 2.04–2.24, mean 2.13; EL/EW = 1.44–1.57, mean 1.50 in four males and three females.

Ventral side (Figures 11F and 12F). Posteromedian area of male sternite VII flat or slightly depressed, slightly elevated longitudinally near middle, apical border sharply intruded internally near middle and tilted toward right side, with microsculpture consisting of narrow to wide transverse irregular meshes (Figure 12F).

Male genitalia (Figures 3K–O and 9E,F). Median lobe of aedeagus (Figure 3K–O) stout, well curved in lateral view, almost linear in dorsal view; ventral side distinctly curved behind basal bulb and gently curved before apex; left lateral margin below apical orifice almost linear; apical orifice bent to left; terminal lamella very short; apex almost truncate; ventral carina distinct, widely rounded; internal sac with three sclerotized areas: (i) gonopore piece on median area, (ii) moderate sized, water drop-shaped ventral sclerite on subapical area, and (iii) spiny patch consisting of numerous sclerotized compact spines subapically; left paramere (Figure 9E) wide, apex truncate; right paramere (Figure 9F) slender, distinctly curved, slightly sinuate before apex.

Type locality. Mt. Yonggusan, Damyang-gun, S. Korea (Figure 1C).

Distribution. See Figure 1C.

Etymology. The specific name "*mixtus*" refers to the morphological characteristic of the new species being intermediate between *P. bifoveolatus* and *P. spinulosus*.

Remarks. This new species externally resembles *P. spinulosus*. The male genital characters, on the other hand, seem to be intermediate between *P. spinulosus* and *P. bifoveolatus*. The stoutness and shape of the carina of the median lobe of the aedeagus resemble those of *P. bifoveolatus*, while the median lobe of the aedeagus with a truncate apex and spiny patch in the internal sac resembles *P. spinulosus*.

Ecology. At the type locality, three field surveys were conducted annually from 2023 to 2025. During these surveys, *P. bifoveolatus* was found sympatrically with the new species. *Pterostichus bifoveolatus* was typically found beneath the bark of the rotten pine tree, whereas the new species was exclusively found under the rocks near a humid valley. Specimens from Mt. Baegasan were also collected under rocks. We suspect that there are differences in ecological niches between the two species.

4.7.5 | *Pterostichus* (*Abea*) *multispinulosus* Kim & Hwang sp. nov.

(Figures 1C, 3P–T, 9G,H, 11G,H and 12G,H)

urn:lsid:zoobank.org:act:86696E45-9215-4053-A3F0-423B70AD0F02

Korean name: 거제꼬마길쭉먼지벌레 [신칭]

Type specimens. *Holotype*: 1♂; GN, Geoje-si, Mundong-dong, Mundong Recreational Forest; alt. ca 240 m; 34°51′38.7″N 128°40′02.0″E; 14.V.2023; Dooyoung Kim (Vial & DNA Voucher No. GJEMicro1). *Paratypes*: 1♂1♀; same data as for holotype (Vial No. GJEMicro2). 8♂4♀; same data as for holotype (Vial No. GJEMicro3–10); 19.V.2024; Dooyoung Kim, Hyejeong Yu. 4♂8♀; same data as for holotype; 26.IV.2025; Dooyoung Kim, Hyejeong Yu (Vial No. GJEMicro11–18). 2♂; GN, Geoje-si, Samgeo-dong, Mt. Seonjasan; alt. ca 270 m; 34°50′55.3″N 128°38′05.7″E; 26.IV.2025; Dooyoung Kim, Hyejeong Yu (Vial No. GJEMicro19–20).

Diagnosis. This species is most similar to *P. spinulosus* and can be best distinguished from it by having three spiny patches in the internal sac of the aedeagus. Other significant characters are as follows.

Pronotum (Figure 12G) with two pairs of basal foveae, outer fovea distinct and rarely faint. Posteromedian area of male sternite VII (Figure 12H) flat, but slightly elevated longitudinally in middle, with microsculpture of irregular polygonal meshes. Median lobe of aedeagus (Figure 3P–T) stout; apex truncate; ventral carina present, widely rounded; sclerotized areas of internal sac consist of the following: (i) gonopore piece on median area, (ii) small, oval-shaped ventral sclerite on subapical area, and (iii) three spiny patches consisting of numerous sclerotized compact spines on dorsal side.

Description. Body length: 6.6–8.1 mm, width: 2.5–3.1 mm.

Coloration (Figure 11G, H) black and shiny; antennae, legs, and lateral margin of pronotum and elytra dark brown; palpi yellowish brown, with apices distinctly paler; ventral side overall black, sternites brownish black.

Head (Figure 12G). Eye moderately convex; tempus slightly developed, weakly convex; frontal impression deep, tilted toward anterior supraorbital pore.

Pronotum (Figure 12G) widest behind 2/5 from apex; apical angle narrowly rounded, slightly protruded anteriorly; lateral margin moderately convex throughout, without sinuation before basal angle; anterolateral seta before widest point, near 1/4 to 3/10 from apex; basal angle slightly to moderately protruded laterally; anterior and posterior transverse impression faint or almost invisible; inner basal foveae deep, linear, almost parallel, with faint or distinct punctures; outer foveae distinct and rarely faint, tilted outward; area between inner foveae with punctures except for median area; area between inner fovea and outer fovea smooth or with faint punctures. PW/HW = 1.59–1.68, mean 1.63; PW/PL

= 1.11–1.18, mean 1.15; PW/PbW = 1.17–1.23, mean 1.21; PW/PaW = 1.41–1.53, mean 1.47; PbW/PaW = 1.19–1.25, mean 1.22 in 10 males and 4 females.

Elytra widest near or behind middle; striae shallow basally, laterally, and apically, slightly deeper medially, punctures distinct from base to basal half; marginal umbilicate series composed of three groups, humeral group with 5 pores, medial group with one pore (rarely two pores), and apical group with seven pores (rarely six or eight pores). EW/PW = 1.12–1.20, mean 1.18; EL/PL = 1.87–2.07, mean 1.95; EL/EW = 1.39–1.50, mean 1.45 in 10 males and 4 females.

Ventral side (Figures 11H and 12H). Posteromedian area of male sternite VII flat, but slightly elevated longitudinally in middle, with microsculpture consisting of irregular polygonal meshes (Figure 12H).

Male genitalia (Figures 3P–T and 9G,H) overall similar to *P. spinulosus*; median lobe of aedeagus (Figure 3P–T) stout, well curved in lateral view, almost linear in dorsal view; ventral side distinctly curved behind basal bulb and gently curved before apex; left lateral margin below apical orifice almost linear; apical orifice bent to left; terminal lamella very short; apex truncate; ventral carina present, widely rounded; internal sac with following sclerotized areas: (i) gonopore piece on median area, (ii) small sized, oval-shaped ventral sclerite on subapical area, and (iii) three spiny patches consisting of numerous sclerotized compact spines on dorsal side; left paramere (Figure 9G) wide, apex truncate; right paramere (Figure 9H) slender, distinctly curved, forming obtuse angle, gradually becomes narrower apically.

Type locality. Mundong recreational forest, Geoje-si, S. Korea (Figure 1C).

Etymology. The specific name "*multispinulosus*" refers to the genital characteristic of the new species.

4.7.6 | *Pterostichus* (*Abea*) *bifoveolatus* Park, Kwon & Lafer, 1996

(Figures 1B, 4A–J, 10A–D, 13A–C and 14A–F)

Korean name: 꼬마길쭉먼지벌레

Pterostichus (*Micronialoe*) *bifoveolatus* Park, Kwon & Lafer, 1996 [71]:74. Type locality: Mt. Jirisan, Gyeongsangnam-do, Korea.

Specimens Examined. DG – 1♂; DG, Dalseong-gun, Gachang-myeon, Ju-ri, Mt. Choejeongsan; alt. ca 550 m; 35°44′38.8″N 128°37′06.8″E; 30.X.2021; Dooyoung Kim (Vial No. CJMB4). 2♂1♀; DG, Dalseong-gun, Gachang-myeon, Ju-ri, Mt. Choejeongsan; alt. ca 350 m; 35°45′08.6″N 128°37′39.8″E; 9.IX.2022; Dooyoung Kim (Vial No. CJMB2, 3). 1♂; DG, Dalseong-gun, Gachang-myeon, Ju-ri, Mt. Choejeongsan; alt. ca 630 m; 35°44′37.4″N 128°36′49.4″E; 9.IX.2022; Dooyoung Kim (Vial & DNA Voucher No. CJMB1). 4♂4♀; DG, Gunwi-gun, Bugye-myeon, Namsan-ri, Mt. Palgongsan; alt. ca 560 m; 36°01′20.4″N 128°38′28.2″E; 1.VI.2024; Dooyoung Kim (Vial No. PGMB1–4). GN – 1♂; GN, Sancheong-gun, Samjang-myeon, Honggye-ri, Bammeorijae Pass; alt. ca 530 m; 35°22′46.7″N 127°51′13.7″E; 5.VIII.2022; Dooyoung Kim (Vial & DNA Voucher No. SCMB1). 1♂; GN, Sancheong-gun; Geumseo-myeon, Sucheol-ri, Mt. Wangsan; alt. ca 450 m; 35°24′14.7″N 127°48′11.5″E; 5.VIII.2022; Dooyoung Kim (Vial & DNA Voucher No. WSMB1). JB – 1♂; JB, Jinan-gun, Jinan-eup, Garim-ri, near Mt. Maisan; alt. ca 430 m; 35°43′57.2″N 127°25′33.7″E; 9.VII.2023; Dooyoung Kim (Vial & DNA Voucher No. MIMB1). JN – 4♂4♀; JN, Gurye-gun, Ganjeon-myeon, Jungdae-ri, Mt. Baegunsan; alt. ca 580 m; 35°07′55.8″N 127°36′12.6″E; 2.IX.2023; Dooyoung Kim (Vial No. BUMB1–5; DNA Voucher No. BUMB1). 10♂5♀; JN, Gurye-gun, Sandong-myeon, Jwasa-ri, Nogodan; alt. ca 1160 m; 35°18′08.0″N 127°30′48.8″E; 25. V.2024; Dooyoung Kim, Hyejeong Yu (Vial No. JRMB1–12; DNA Voucher No. JRMB1). 6♂7♀; JN, Damyang-gun, Weolsan-myeon, Yongheung-ri, Mt. Yonggusan; alt. ca 370 m; 35°20′12.9″N 126°53′40.7″E; 6.VII.2024; Dooyoung Kim (Vial No. DYMB1–7). 1♂; same data as for preceding; 31. V.2025; Dooyoung Kim, Hyejeong Yu (Vial No. DYMB8).

Diagnosis and Redescription. See Kim and Suh [2].

Measurements. Body length: 6.3–9.1 mm; body width: 2.3–3.3 mm; PW/HW = 1.54–1.70, mean 1.63; PW/PL = 1.09–1.24, mean 1.15; PW/PbW = 1.11–1.26, mean 1.17; PW/PaW = 1.33–1.48, mean 1.42; PbW/PaW = 1.13–1.31, mean 1.21; EW/PW = 1.12–1.24, mean 1.19; EL/PL = 1.94–2.26, mean 2.10; EL/EW = 1.44–1.66, mean 1.54 in 30 males and 22 females.

Distribution. It is widely distributed across the southern part of South Korea (Figure 1B).

Variations. In general, there are distinct punctations on or near the basal fovea in this species. However, some specimens from Mt. Baegunsan (JN) either lack these punctures or exhibit them only faintly. The modification in the posteromedian area of the male sternite VII is usually with a transverse depression before the apical margin and a longitudinal depression on the right side (Figure 14B). In contrast, specimens from Mt. Palgongsan (DG), Mt. Choejeongsan (DG), and Mt. Yonggusan (JN) had a longitudinal depression in the middle (Figure 14D).

The most unique form was collected from Mt. Wangsan (GN) (Figures 13C, 14E,F, 4F–J, and 10C, D). Though this place was close to the type locality of the species, it had some different features compared with typical forms: (i) eye smaller and flatter (Figure 14E), (ii) apical angle of pronotum narrowly rounded and distinctly protruded anteriorly (Figure 14E), (iii) surface of the male sternite VII shallowly depressed in posteromedian area (Figure 14F), (iv) carina on median lobe of aedeagus distinctly narrowly rounded (Figure 4G), and (v) ventral sclerite wider apically (Figure 4I). The general body form of this locality superficially resembles *P. subterraneus*. It seems that this specimen is an intermediate adaptation form of a subterranean habitat.

Ecology. The members are sometimes found sympatrically with other species: (i) with *P. chogyesanus* in Mt. Jirisan (JN) and Mt. Baegunsan (JN); (ii) with *P. spinulosus* in Mt. Choejeongsan (DG) and Mt. Palgongsan (DG); (iii) with *P. mixtus* in Mt. Yonggusan (JN). This species was found under the bark of rotten trees in Mt. Yonggusan, near Mt. Maisan (JB), and Mt. Palgongsan.

4.7.7 | *Pterostichus* (*Abea*) *spinulosus* Kim & Suh, 2024

(Figures 1C, 4K–T, 10E–H, 13D,E and 14G–J)

Korean name: 주름꼬마길쭉먼지벌레

Pterostichus (*Micronialoe*) *spinulosus* Kim & Suh, 2024 [2]:454. Type locality: Mt. Biseulsan and Mt. Choejeongsan, Daegu-si, Korea.

Specimens Examined (Morphotype 7, Genital Type With Spiny Patch on Dorsal Side as in Type Series). 1♂; DG, Dalseong-gun, Gachang-myeon, Jeongdae-ri, Eastern part of Mt. Biseulsan; alt. ca 500 m; 35°43′48.1″N 128°33′06.5″E; 29.X.2021; Dooyoung Kim; holotype (Vial No. BSMicro1). 3♂2♀; DG, Dalseong-gun, Gachang-myeon, Jeongdae-ri, Eastern part of Mt. Biseulsan; alt. ca 500 m; 35°43′48.1″N 128°33′06.5″E; 29.X.2021; Dooyoung Kim; paratypes (Vial No. BSMicro2–6). 10♂2♀ DG, Dalseong-gun, Gachang-myeon, Jeongdae-ri, Eastern part of Mt. Biseulsan; alt. ca 580 m; 35°43′30.8″N 128°32′33.1″E; 26.VI.2021; Dooyoung Kim; paratypes (Vial No. BSMicro7–18; DNA Voucher No. BSMicro8). 4♂1♀; DG, Dalseong-gun, Gachang-myeon, Jeongdae-ri, Eastern part of Mt. Biseulsan; alt. ca 500 m; 35°43′48.1″N 128°33′06.5″E; 16.V.2021; Dooyoung Kim; paratypes (Vial No. BSMicro19–23). 1♂; DG, Dalseong-gun, Gachang-myeon, Ju-ri, Mt. Choejeongsan; alt. ca 800 m; 35°45′14.4″N 128°35′59.6″E; 1.VII.2021; Dooyoung Kim; paratype (Vial & DNA Voucher No. CJMicro1). 1♂; DG, Dalseong-gun, Gachang-myeon, Ju-ri, Mt. Choejeongsan; alt. ca 900 m; 35°45′46.3″N 128°36′05.5″E; 25.VI.2024; Dooyoung Kim (Vial & DNA Voucher No. CJMicro2). 1♂; DG, Dalseong-gun, Gachang-myeon, Ju-ri, Mt. Choejeongsan; alt. ca 900 m; 35°45′46.3″N 128°36′05.5″E; 28.IX.2024; Dooyoung Kim (Vial No. CJMicro3). 6♂2♀; DG, Dalseong-gun, Gachang-myeon, Ju-ri, Mt. Choejeongsan; alt. ca 900 m; 35°45′46.3″N 128°36′05.5″E; 29.VI.2024; Dooyoung Kim (Vial No. CJMicro4–9). 25♂15♀; DG, Gunwi-gun, Bugye-myeon, Namsan-ri, Mt. Palgongsan; alt. ca 560 m; 36°01′20.4″N 128°38′28.2″E; 1.VI.2024; Dooyoung Kim (Vial No. PGMicro4–19).

Additional Specimens Examined (Morphotype 8, Genital Type With Spiny Patch on Apical Side). 10♂; GB, Yeongcheon-si, Sinnyeong-myeon, Hwanam-ri, Mt. Hwasan, alt. ca 680 m; 36°05′37.0″N 128°47′09.5″E; 2.VII.2022; Dooyoung Kim (Vial No. HSMicro1–10; DNA Voucher No. HSMicro1). 2♂3♀; GN, Yangsan-si, Habuk-myeon, Yongyeon-ri, Mt. Cheonseongsan; alt. ca 220 m; 35°23′28.0″N 129°05′08.2″E; 22.IV.2023; Dooyoung Kim (Vial No. YSAMicro1–3). 2♂1♀; DG, Gunwi-gun, Bugye-myeon, Dongsan-ri, Mt. Palgongsan; alt. ca 500 m; 36°02′03.0″N 128°40′08.9″E; 12.V.2023; Dooyoung Kim (Vial No. PGMicro1–3; DNA Voucher No. PGMicro1). 6♂1♀; US, Ulju-gun, Sangbuk-myeon, Soho-ri, Mt. Goheonsan; alt. ca 570 m; 35°39′18.8″N 129°05′02.0″E; 8.VII.2023; Dooyoung Kim (Vial No. GHMicro1–6; DNA Voucher No. GHMicro1). 3♂2♀; PS, Saha-gu, Dangri-dong, Mt. Seunghaksan; alt. ca 190 m; 35°06′53.9″N 128°59′19.2″E; 1.IV.2025; Hyejeong Yu (Vial No. BUSMicro1–3).

Diagnosis and Redescription. See Kim and Suh [2].

Measurements. Body length: 6.4–8.3 mm; body width: 2.4–3.0 mm; PW/HW = 1.51–1.70, mean 1.62; PW/PL = 1.09–1.24, mean 1.16; PW/PbW = 1.14–1.21, mean 1.18; PW/PaW = 1.39–1.55, mean 1.47; PbW/PaW = 1.17–1.32, mean 1.25; EW/PW = 1.11–1.27, mean 1.18; EL/PL = 1.84–2.13, mean 1.99; EL/EW = 1.33–1.58, mean 1.47 in 45 males and 15 females.

Distribution. See Figure 1C.

Variations. The specimens collected from Gyeongsangnam-do and the southern Gyeongsangbuk-do, which are not far from the type locality, have different features in the median lobe of the aedeagus. Their spiny patch in the median lobe of the aedeagus was consistently placed near the subapical part (Morphotype 8; Figure 4K–T), different from *P. spinulosus* collected from the type locality, which has a spiny patch on its dorsal side. The new genital form seems to be more widely spread than the original type (Figure 1C).

Interestingly, both genital forms were observed from Mt. Palgongsan (DG), located slightly north of the type locality. The specimens collected from the northwestern part were identical to those of the type locality, and those from the northern part were identical to the newly identified form. Even though the collection sites of the two forms are closely located on Mt. Palgongsan, they were not found to be mixed. Since there are no distinct natural barriers between the two populations, there must be a region where those two forms are sympatric.

4.7.8 | *Pterostichus* (*Abea*) *chogyesanus* Park, Kwon & Lafer, 1996

(Figures 1C and 10I–L)

Korean name: 송광길쭉먼지벌레

Pterostichus (*Micronialoe*) *chogyesanus* Park, Kwon & Lafer, 1996 [71]:75. Type locality: Mt. Jogyesan, Suncheon-si, Korea.

Specimens examined. 5♂; JN, Gurye-gun, Ganjeon-myeon, Jungdae-ri; Mt. Baegunsan; alt. ca 580 m; 35°07′55.8″N 127°36′12.6″E; 3.IX.2022; Dooyoung Kim (Vial No. BUMC1–5; DNA Voucher No. BUMC1). 8♂7♀; JN, Gurye-gun, Sandong-myeon, Jwasa-ri, Nogodan; alt. ca 1160 m; 35°18′08.0″N 127°30′48.8″E; 25.V.2024; Dooyoung Kim, Hyejeong Yu (Vial No. JRMC1–8; DNA Voucher No. JRMC1).

Other specimens examined. 1♀; JN, Hwasun-gun, Baega-myeon, Songdan-ri, Mt. Baegasan; alt. ca 480 m; 35°10′4.8″N 127°11′10.3″E; 6.VII.2024; Dooyoung Kim (Vial No. HSUMC1).

Diagnosis and Redescription. See Kim and Suh [2].

Measurements. Body length: 5.1–6.3 mm; body width: 2.0–2.3 mm; PW/HW = 1.48–1.58, mean 1.51; PW/PL = 1.10–1.19, mean 1.15; PW/PbW = 1.21–1.31, mean 1.26; PW/PaW = 1.40–1.50, mean 1.44; PbW/PaW = 1.07–1.20, mean 1.15; EW/PW = 1.16–1.28, mean 1.23; EL/PL = 2.00–2.18, mean 2.06; EL/EW = 1.39–1.56, mean 1.46 in 12 males and 7 females.

Distribution. It has only been found in Mt. Jogyesan, Mt. Baegunsan, and Mt. Jirisan (Figure 1C).

Variations. Its variation in the right paramere was observed within the population. The apical part is sometimes distinctly curved, but sometimes almost linear (Figure 10I–L). The morphometric measurement of a female specimen from Mt. Baegasan (JN) fits into the range of *P. chogyesanus*.

4.7.9 | Key to the Species of the Subgenus *Abea* (Also See Table 2 for Korean Species)

1. Eye almost reduced; mentum with additional setae near a pair of pit……*P. subterraneus* sp. nov.
– Eye present, distinct; mentum without additional setae……2.
2. Body length at most 6.6 mm; PW/HW < 1.58; PW/PbW > 1.21; median lobe of aedeagus slender or stout, apical orifice on dorsal side or bent to left…… 3.
– Body length larger than 6.0 mm; PW/HW > 1.53; PW/PbW < 1.28; median lobe of aedeagus stout, apical orifice bent to left…… 4.
3. Median lobe of aedeagus rather slender, apical orifice on dorsal side; distributed in Mt. Jogyesan and nearby regions, Korea……*P. chogyesanus* Park, Kwon & Lafer.
– Median lobe of aedeagus stout, apical orifice bent to left; distributed in Aomori Prefecture and nearby regions, Japan ……*P. yamauchii* Morita.
4. Median lobe of aedeagus truncate at apex in dorsal view, internal sac with one or more spiny patches……5.
– Median lobe of aedeagus rounded at apex in dorsal view, internal sac without spiny patches (sclerotized parts for *P.* (*M.*) *kaniei* are unknown)……7.
5. Internal sac with three spiny patches……*P. multispinulosus* sp. nov.
– Internal sac with one spiny patch……6.
6. Apical border of male abdominal sternite VII sharply intruded in the middle; median lobe of aedeagus relatively stout, ventral sclerite larger……*P. mixtus* sp. nov.
– Apical border of male abdominal sternite VII without modification; median lobe of aedeagus relatively slender, ventral sclerite smaller……*P. spinulosus* Kim & Suh.
7. Median lobe of aedeagus without carina……*P. bifoveolatoides* sp. nov.
– Median lobe of aedeagus with carina……8.
8. Pronotum with vague outer basal fovea; smaller species (6.1–7.0 mm); distributed in Is. Tsushima, Japan……*P. kaniei* Morita.
– Pronotum with distinct outer basal fovea; larger species (generally > 7.0 mm); distributed in Mt. Jirisan, Korea……*P. bifoveolatus* Park, Kwon & Lafer.

Remarks. This species key does not fully work for female specimens. Based on current knowledge, distribution information could become a good prior source for identification when only females are collected, for example, *P. bifoveolatoides* is only known from the northern part of South Korea, whose range only overlaps with morphologically distinct *P. subterraneus*. In the southern part of South Korea, *P. bifoveolatus* is frequently observed with other species. In general, this species can be differentiated from co-occurring species through relatively strong punctures near the basal foveae. On the other hand, the population of this species in Mt. Baegunsan (JN) had weak pronotal punctures, but the co-occurring *P. chogyesanus* can be easily distinguished through the above key. Still, there could be undiscovered species as well as unidentified species pairs, so classifying females without male specimens is a challenge.

5 | Conclusion

We investigated the phylogenetic relationships of *Abea* and related subgenera, proposed the synonymy of *Micronialoe*, and reconstructed the biogeographical history of the group. Our results suggested that *Abea* likely dispersed from southern China, followed by subsequent dispersal to the Korean Peninsula and the Japanese Archipelago. Looking ahead, comprehensive revisionary work will be essential for the genus *Pterostichus*, which currently includes ~90 proposed subgenera [72], many of which are small or monotypic. These groups require re-examination using integrative approaches to establish a more robust supraspecific classification. Moreover, because *Pterostichus* is widely distributed and many of its subgenera exhibit regional endemism, expanded molecular sampling across the genus will provide valuable insights into its large-scale biogeographical history with greater accuracy.

By incorporating specimens from both known and newly surveyed localities, this work fills important sampling gaps and provides a comprehensive overview of *Abea* in South Korea. The discovery of four new species was supported by a combination of molecular data and male genital morphology. However, morphometric analyses did not clearly differentiate species, complicating the identification of teneral and female specimens. Future research should prioritize surveys in poorly investigated regions and subterranean habitats, while continuing to apply integrative approaches. Such efforts will further clarify the biodiversity and evolutionary history of the group.

Acknowledgments

The authors would like to express a sincere appreciation to Mr. Seiji Morita (Tokyo, Japan) for providing valuable information on the Japanese *Micronialoe* and *Abea*. We heartfully appreciate Ms. Hyejeong Yu and Mr. Gyeongmin Kim for collaborating in field surveys, and Mr. Geonhyeok Kim and Mr. Yongtae Jang for providing a valuable *Abea* specimen from Korea. We are grateful to Mr. Yong-Gun Choi (The Korean Institute of Biospeleology, Daejeon, Korea) and the members of the Korean Society of Cave Environmental Science for assisting cave research. Furthermore, we thank the anonymous reviewers for their valuable comments during the review process. We acknowledge the use of ChatGPT-5 for grammatical review and improving the manuscript's readability.

Funding

This work was supported by a grant for UWH from the National Institute of Biological Resources (NIBR), funded by the Ministry of Environment (MOE), Republic of Korea (NIBRE202405), and from the National Research Foundation of Korea (NRF) under the Ministry of Science and ICT (MSIT), Republic of Korea (RS-2025-00561309).

Conflicts of Interest

The authors declare no conflicts of interest.

Data Availability Statement

The sequence data generated in this study have been deposited in GenBank under accession numbers PV954984–PV955010 and PV955577–PV955597. The data that support the findings of this study are openly available in Open Science Framework at https://osf.io/yeu47/?view_only=2fe6dd518f3e4f93878f5ccd7632f74b.

References

1. S. Morita, "A New Subgenus and Species of *Pterostichus* (Coleoptera, Carabidae) From Aomori Prefecture, North Japan," *Elytra* 20 (1992): 15–19.

2. D. Kim and S. J. Suh, "Review of the Ground Beetle Subgenus *Micronialoe* From Korea, With a Description of a New Species (Coleoptera: Carabidae: *Pterostichus*)," *Zootaxa* 5471, no. 4 (2024): 451–464.

3. S. Morita, "A New *Pterostichus* (Coleoptera: Carabidae) From the Islands of Tsushima, West Japan," *Entomological Review of Japan* 60, no. 1 (2005): 9–12.

4. K. Sasakawa and K. Kubota, "Phylogeny and Genital Evolution of Carabid Beetles in the Genus *Pterostichus* and Its Allied Genera (Coleoptera: Carabidae) Inferred From Two Nuclear Gene Sequences," *Annals of the Entomological Society of America* 100, no. 2 (2007): 100–109.

5. K. W. Will and A. S. Gill, "Phylogeny and Classification of *Hypherpes auctorum* (Coleoptera: Carabidae: Pterostichini: *Pterostichus*)," *Annals of Carnegie Museum* 77, no. 1 (2008): 93–127.

6. J. Schmidt, L. Opgenoorth, S. Höll, R. Bastrop, and R. DeSalle, "Into the Himalayan Exile: The Phylogeography of the Ground Beetle *Ethira* clade Supports the Tibetan Origin of Forest-Dwelling Himalayan Species Groups," *PLoS ONE* 7, no. 9 (2012): e45482.

7. P. D. N. Hebert, A. Cywinska, S. L. Ball, and J. R. deWaard, "Biological Identifications Through DNA Barcodes," *Proceedings of the Royal Society of London. Series B: Biological Sciences* 270, no. 1512 (2003): 313–321.

8. U. Jinbo, T. Kato, and M. Ito, "Current Progress in DNA Barcoding and Future Implications for Entomology," *Entomological Science* 14, no. 2 (2011): 107–124.

9. M. J. Raupach, K. Hannig, J. Morinière, and L. Hendrich, "A DNA Barcode Library for Ground Beetles of Germany: The Genus, *Pterostichus*, Bonelli, 1810 and Allied Taxa (Insecta, Coleoptera, Carabidae)," *ZooKeys* 980 (2020): 93–117.

10. N. A. Zubrii, B. Y. Filippov, A. V. Kondakov, O. A. Khruleva, and L. B. Rybalov, "Integrative Taxonomy of Two Morphologically Similar Species of the Subgenus, *Cryobius*, Chaudoir, 1838 (Coleoptera: Carabidae: *Pterostichus*, Bonelli, 1810) From Northern Eurasia and North America," *Ecologica Montenegrina* 61 (2023): 8–15.

11. K. Sasakawa and K. Kubota, "Utility of External Morphometrics for Cryptic Species Identification: A Case Study of Two Species in *Poecilus* '*samurai*' (Coleoptera: Carabidae)," *Applied Entomology and Zoology* 42, no. 3 (2007): 353–365.

12. C. Huber and P. H. Schnitter, "*Nebria* (*Pseudonebriola*) *tsambagarav* sp. nov., a New Alpine Species From the Mongolian Altai (Coleoptera, Carabidae)," *Alpine Entomology* 4 (2020): 29–38.

13. K. Sasakawa, "Two New Species of the Ground Beetle Subgenus, *Sadonebria*, Ledoux & Roux, 2005 (Coleoptera, Carabidae, *Nebria*) From Japan and First Description of Larvae of the Subgenus," *ZooKeys* 578 (2016): 97–113.

14. A. Roggero, P. M. Giachino, A. Casale, G. Allegro, A. Fiorito, and C. Palestrini, "Combination of Morphometric and Morphological Analyses: An Effective Approach for the Study of *Platynus* From the Italian W Alps (Coleoptera, Carabidae, Platynini)," *Diversity* 15, no. 4 (2023): 493.

15. K. Sasakawa and Y. Mitsuduka, "A Morphology-Based Revision and Phylogenetic Analysis of the *Pterostichus macrogenys* Species Group (Coleoptera, Carabidae) and Implications for Differentiation of the Species Group," *Deutsche Entomologische Zeitschrift* 70, no. 2 (2023): 291–310.

16. A. Habu, *Fauna Japonica. Carabidae: Platynini (Insecta: Coleoptera)* (Keigaku Publishing Co Ltd., 1978).

17. T. Sota, *Evolutionary Biology of Carabus Ground Beetles: How Species Richness Increases* (Springer Nature, 2021).

18. K. A. Ober, "Phylogenetic Relationships of the Carabid Subfamily Harpalinae (Coleoptera) Based on Molecular Sequence Data," *Molecular Phylogenetics and Evolution* 24, no. 2 (2002): 228–248.

19. O. Folmer, M. Black, W. Hoeh, R. Lutz, and R. Vrijenhoek, "DNA Primers for Amplification of Mitochondrial Cytochrome c Oxidase Subunit I From Diverse Metazoan Invertebrates," *Molecular Marine Biology and Biotechnology* 3, no. 5 (1994): 294–299.

20. K. Sasakawa and K. Kubota, "Phylogeny of Ground Beetles Subgenus *Nialoe* (*s. lat.*) Tanaka (Coleoptera: Carabidae; Genus *Pterostichus*): A Molecular Phylogenetic Approach," *Entomological Science* 12, no. 3 (2009): 308–313.

21. D. D. McKenna, A. L. Wild, K. Kanda, et al., "The Beetle Tree of Life Reveals that Coleoptera Survived End-Permian Mass Extinction to Diversify During the Cretaceous Terrestrial Revolution," *Systematic Entomology* 40, no. 4 (2015): 835–880.

22. A. Faille, A. Casale, C. Hernando, S. Aït Mouloud, and I. Ribera, "Tectonic Vicariance Versus Messinian Dispersal in Western Mediterranean Ground Beetles," *Zoologica Scripta* 47, no. 5 (2018): 565–581.

23. J. D. Thompson, D. G. Higgins, and T. J. Gibson, "CLUSTALW: Improving the Sensitivity of Progressive Multiple Sequence Alignment Through Sequence Weighting, Position-Specific Gap Penalties and Weight Matrix Choice," *Nucleic Acids Research* 22, no. 22 (1994): 4673–4680.

24. T. A. Hall, "BioEdit: A User-Friendly Biological Sequence Alignment Editor and Analysis Program for Windows 95/98/NT," *Nucleic Acids Symposium Series* 41 (1999): 95–98.

25. K. Katoh, J. Rozewicki, and K. D. Yamada, "MAFFT Online Service: Multiple Sequence Alignment, Interactive Sequence Choice and Visualization," *Briefings in Bioinformatics* 20, no. 4 (2019): 1160–1166.

26. G. Talavera, J. Castresana, K. Kjer, R. Page, and J. Sullivan, "Improvement of Phylogenies After Removing Divergent and Ambiguously Aligned Blocks From Protein Sequence Alignments," *Systematic Biology* 56, no. 4 (2007): 564–577.

27. W. P. Maddison and D. R. Maddison, "Mesquite: A Modular System for Evolutionary Analysis," 2025, https://www.mesquiteproject.org/ Version 3.81. [accessed 2025 Feb 2].

28. D. H. Kavanaugh, D. R. Maddison, W. B. Simison, et al., "Phylogeny of the Supertribe Nebriitae (Coleoptera, Carabidae) Based on Analyses of DNA Sequence Data," *ZooKeys* 1044 (2021): 41–152.

29. J. Trifinopoulos, L.-T. Nguyen, A. von Haeseler, and B. Q. Minh, "W-IQ-TREE: A Fast Online Phylogenetic Tool for Maximum Likelihood Analysis," *Nucleic Acids Research* 44, no. W1 (2016): W232–W235.

30. S. Kalyaanamoorthy, B. Q. Minh, T. K. F. Wong, A. von Haeseler, and L. S. Jermiin, "ModelFinder: Fast Model Selection for Accurate Phylogenetic Estimates," *Nature Methods* 14, no. 6 (2017): 587–589.

31. O. Chernomor, A. Von Haeseler, and B. Q. Minh, "Terrace Aware Data Structure for Phylogenomic Inference From Supermatrices," *Systematic Biology* 65, no. 6 (2016): 997–1008.

32. D. T. Hoang, O. Chernomor, A. Von Haeseler, B. Q. Minh, and L. S. Vinh, "UFBoot2: Improving the Ultrafast Bootstrap Approximation," *Molecular Biology and Evolution* 35, no. 2 (2018): 518–522.

33. F. Ronquist, M. Teslenko, P. Van Der Mark, et al., "MrBayes 3.2: Efficient Bayesian Phylogenetic Inference and Model Choice Across a Large Model Space," *Systematic Biology* 61, no. 3 (2012): 539–542.

34. R. Bouckaert, J. Heled, D. Kühnert, et al., "BEAST. 2: A Software Platform for Bayesian Evolutionary Analysis," *PLoS Computational Biology* 10, no. 4 (2014): e1003537.

35. T. Gernhard, "The Conditioned Reconstructed Process," *Journal of Theoretical Biology* 253, no. 4 (2008): 769–778.

36. J. Douglas, R. Zhang, R. Bouckaert, and R. D. Kouyos, "Adaptive Dating and Fast Proposals: Revisiting the Phylogenetic Relaxed Clock Model," *PLoS Computational Biology* 17, no. 2 (2021): e1008322.

37. A. Rambaut, A. J. Drummond, D. Xie, G. Baele, M. A. Suchard, and E. Susko, "Posterior Summarization in Bayesian Phylogenetics Using Tracer 1.7," *Systematic Biology* 67, no. 5 (2018): 901–904.

38. A. Rambaut, "FigTree v1.4.4," 2018, http://tree.bio.ed.ac.uk/software/figtree/ 2025-09-01.

39. Y. Yu, A. J. Harris, C. Blair, and X. He, "RASP (Reconstruct Ancestral State in Phylogenies): A Tool for Historical Biogeography," *Molecular Phylogenetics and Evolution* 87 (2015): 46–49.

40. H. Yoshitake, T. Kurihara, S. Yoshimatsu, Y. Nakatani, and K. Yasuda, "A List of Carabid Specimens (Insecta: Coleoptera) Collected by the Late Dr. Akinobu Habu Preserved in the Insect Museum of the National Institute for Agro-Environmental Sciences," *Bulletin of the National Institute of Agricultural Sciences Series C* 28 (2011): 1–327, [in Japanese with English summary].

41. H. Shi and H. Liang, "The Genus *Pterostichus* in China II: The Subgenus, *Circinatus*, Sciaky, A Species Revision and Phylogeny (Carabidae, Pterostichini)," *ZooKeys* 536 (2015): 1–92.

42. S. Yoshimatsu, N. Ito, Y. Nakatani, and H. Yoshitake, "A List of Ground Beetles (Insecta: Coleoptera: Caraboidea) in Dr. Kazuo Tanaka Collection Preserved in the Insect Museum of Institute for Agro-Environmental Sciences, NARO," *Bulletin of the National Institute of Agro-Environmental Sciences* 39 (2018): 15–191, [in Japanese].

43. S. Kumar, G. Stecher, M. Suleski, M. Sanderford, S. Sharma, and K. Tamura, "Molecular Evolutionary Genetics Analysis Version 12 for Adaptive and Green Computing," *Molecular Biology and Evolution* 41, no. 12 (2024): 1–9.

44. M. Kimura, "A Simple Method for Estimating Evolutionary Rate of Base Substitutions Through Comparative Studies of Nucleotide Sequences," *Journal of Molecular Evolution* 16, no. 2 (1980): 111–120.

45. R Core Team, "R: A Language and Environment for Statistical Computing," (2025).

46. R Studio Team, "RStudio: Integrated Development for R," (PBC (2025).

47. H. Wickham, *ggplot2: Elegant Graphics for Data Analysis* (Springer-Verlag, 2016).

48. H. Wickham and M. H. Wickham, "Package 'Tidyr'. Easily Tidy Data With' Spread'and'gather (.)'Functions," (2017).

49. H. Wickham, R. François, L. Henry, K. Müller, and D. Vaughan, "dplyr: A Grammar of Data Manipulation," 2023, R package version 1.1.4 https://github.com/tidyverse/dplyr, https://dplyr.tidyverse.org.

50. B. Ripley, B. Venables, D. M. Bates, et al., "Package 'Mass," *Cran R* 538 (2013): 113–120.

51. Y.-I. Otofuji, T. Matsuda, and S. Nohda, "Opening Mode of the Japan Sea Inferred From the Palaeomagnetism of the Japan ARC," *Nature* 317, no. 6038 (1985): 603-604.

52. S. Osozawa, R. Shinjo, A. Armid, Y. Watanabe, T. Horiguchi, and J. Wakabayashi, "Palaeogeographic Reconstruction of the 1.55 Ma Synchronous Isolation of the Ryukyu Islands, Japan, and Taiwan and Inflow of the Kuroshio Warm Current," *International Geology Review* 54, no. 12 (2012): 1369–1388.

53. K. Tojo, K. Sekiné, M. Takenaka, et al., "Species Diversity of Insects in Japan: Their Origins and Diversification Processes," *Entomological Science* 20, no. 1 (2017): 357–381.

54. R. Sciaky, "*Sinosteropus* New Subgenus and Three New Species of *Pterostichus* From China (Coleoptera Carabidae)," *Natura Bresciana* 29 (1994): 193–201.

55. S. Facchini and R. Sciaky, "Revision of the, *Pterostichus*, Bonelli, 1810 subg. *Pseudohaptoderus*, Tschitscherine, 1888 and Description of New Taxa (Coleoptera: Carabidae, Pterostichinae)," *Koleopterologische Rundschau* 70 (2000): 1–10.

56. H. Shi, R. Sciaky, H. Liang, and H. Zhou, "A New Subgenus *Wraseiellus* of the Genus, *Pterostichus*, Bonelli (Coleoptera, Carabidae, Pterostichini) and New Species Descriptions," *Zootaxa* 3664, no. 2 (2013): 101–135.

57. X. Jia, L. He, and M. Tian, "A New Subgenus and Three New Cavernicolous Species of the Genus *Pterostichus* From China (Coleoptera: Carabidae: Pterostichini)," *Annales de la Société Entomologique de France, (NS)* 57, no. 4 (2021): 346–358.

58. G. Allegro and P. M. Giachino, "*Abacaecus* n. gen. *walterrossii* n. sp., a Notable Hypogean Carabid Species From Sierra Leone, Western Africa (Coleoptera, Carabidae, Pterostichinae)," *Zootaxa* 4766, no. 3 (2020): 435–446.

59. A. Habu, "*Yukihikous minobusanus*, gen. et sp. nov. (Platynini), From Central Honshu, Japan," *Entomological Review of Japan* 32 (1978): 101–106.

60. S. Morita, "Two New *Yukihikous* (Coleoptera, Carabidae) From Central Japan," *Elytra* 2, no. 2 (2012): 311–318.

61. R. Sciaky, "New Subgenera and New Species of Pterostichini From China (Coleoptera, Carabidae)," *Bollettino del Museo Civico di Storia Naturale di Venezia* 47 (1997): 153–176.

62. J. Li, C. Fu, G. Lei, and D. Nogues-Bravo, "Biogeographical Consequences of Cenozoic Tectonic Events Within East Asian Margins: A Case Study of *Hynobius* Biogeography," *PLoS ONE* 6, no. 6 (2011): e21506.

63. C. W. Oh, "A New Concept on Tectonic Correlation Between Korea, China and Japan: Histories From the Late Proterozoic to Cretaceous," *Gondwana Research* 9, no. 1-2 (2006): 47–61.

64. X. Lin, M. Dröllner, M. Barham, et al., "The Cenozoic Evolution of the Yellow River," *Earth-Science Reviews* 261 (2025): 104997.

65. H. W. Bates, "XI. *Supplement to the Geodephagous Coleoptera of Japan*, *Chiefly From the Collection of* Mr. George Lewis, *Made During his Second Visit*, *From February*, 1880, *to September*, 1881," *Transactions of the Royal Entomological Society of London* 31, no. 3 (1883): 205–290.

66. D. N. Fedorenko, "Notes on *Pterostichus* subgenus, *Steropanus*, Fairmaire, 1889 (Coleoptera: Carabidae: Pterostichini), With Descriptions of New Species," *Russian Entomological Journal* 27, no. 1 (2018): 107–121.

67. D. N. Fedorenko, "A Review of *Pterostichus* subgenus *Orientostichus* (Coleoptera: Carabidae: Pterostichini) From Indochina, With Description of New Species," *Euroasian Entomological Journal* 32, no. 2 (2023): 155–170.

68. R. Shiiba, "Revision of *Pterostichus* (*Sphodroferonia*) *hisamatsui*, Ishida and Shibata and Its Relatives (Coleoptera: Carabidae) From Shikoku and Kyushu," *Japanese Journal of Systematic Entomology* 29, no. 1 (2023): 109–137.

69. W. Q. Yin, J. H. Chen, and H. L. Shi, "Revision of the Chinese Endemic Subgenus, *Tschitscherinea*, Berg, With Descriptions of Three New Species (Coleoptera, Carabidae)," *Zootaxa* 5481, no. 1 (2024): 43–65.

70. B. Guéorguiev, "Three New Species of *Pterostichus* From Myanmar and Vietnam (Coleoptera: Carabidae: Pterostichini)," *Journal of Insect Biodiversity* 58, no. 2 (2024): 39–60.

71. J. K. Park, Y. J. Kwon, and G. S. Lafer, "Classification of the Genus, *Pterostichus*, Bonelli From Korea (Coleoptera: Harpalidae) I. *Micronialoe* Subgen. Nov." *Korean Journal of Entomology* 26 (1996): 72–77.

72. A. Anichtchenko, "Carabidae of the World," 2025, http://carabidae.org.

Supporting Information

Additional supporting information can be found online in the Supporting Information section. **Supporting Information 1**. Table S1. Species information and dataset inclusion for phylogenetic and genetic distance analyses. **Supporting Information 2**. Table S2. Morphometric data and collection information of measured specimens. Abbreviations: SP1: *P. subterraneus*; SP2: *P. bifoveolatoides*: SP3: *P. bifoveolatus*; SP4: *P. chogyesanus*; SP5: *P. mixtus*; SP6: *P. multispinulosus*; SP7: *P. spinulosus*. **Supporting Information 3**. Table S3. Eigenvalues of the principal component analysis (PCA). **Supporting Information 4**. Table S4. Character loadings of the discriminant axes based on the scaled data of the linear discriminant analyses (LDA).